Bioactive Materials 6 (2021) 4286–4300

Contents lists available at ScienceDirect

Bioactive Materials

journal homepage: www.sciencedirect.com/journal/bioactive-materials

Multiplexed detection and differentiation of bacterial enzymes and bacteria by color-encoded sensor hydrogels

Zhiyuan Jia [a], Mareike Müller [a], Tony Le Gall [b], Martijn Riool [c], Max Müller [a], Sebastian A. J. Zaat [c], Tristan Montier [b,d], Holger Schönherr [a,*]

[a] Physical Chemistry I & Research Center of Micro and Nanochemistry and Engineering (Cμ), Department of Chemistry and Biology, University of Siegen, Adolf-Reichwein-Straße 2, 57076, Siegen, Germany
[b] Univ Brest, INSERM, EFS, UMR 1078 GGFB, F-29200, Brest, France
[c] Department of Medical Microbiology and Infection Prevention, Amsterdam institute for Infection and Immunity, Amsterdam UMC, University of Amsterdam, Meibergdreef 9, 1105, AZ, Amsterdam, the Netherlands
[d] CHRU de Brest, Service de génétique médicale et de biologie de la reproduction, Centre de Référence des Maladies Rares « Maladies neuromusculaires », F-29200, Brest, France

ARTICLE INFO

Keywords:
Multiplexed biosensors
Bacteria detection
Bacterial enzyme
Reporter hydrogels
Colorimetric substrates

ABSTRACT

We report on the fabrication and characterization of color-encoded chitosan hydrogels for the rapid, sensitive and specific detection of bacterial enzymes as well as the selective detection of a set of tested bacteria through characteristic enzyme reactions. These patterned sensor hydrogels are functionalized with three different colorimetric enzyme substrates affording the multiplexed detection and differentiation of α-glucosidase, β-galactosidase and β-glucuronidase. The limits of detection of the hydrogels for an observation time of 60 min using a conventional microplate reader correspond to concentrations of 0.2, 3.4 and 4.5 nM of these enzymes, respectively. Based on their different enzyme expression patterns, *Staphylococcus aureus* strain RN4220, methicillin-resistant *S. aureus* (MRSA) strain N315, both producing α-glucosidase, but not β-glucuronidase and β-galactosidase, *Escherichia coli* strain DH5α, producing β-glucuronidase and α-glucosidase, but not β-galactosidase, and the enterohemorrhagic *E. coli* (EHEC) strain E32511, producing β-galactosidase, but none of the other two enzymes, can be reliably and rapidly distinguished from each other. These results confirm the applicability of enzyme sensing hydrogels for the detection and discrimination of specific enzymes to facilitate differentiation of bacterial strains. Patterned hydrogels thus possess the potential to be further refined as detection units of a multiplexed format to identify certain bacteria for future application in point-of-care microbiological diagnostics in food safety and medical settings.

1. Introduction

The World Health Organization reported in 2017 that antibiotic resistance is one of the biggest threats to global health with multidrug-resistant *Enterobacteriaceae,* including *Escherichia coli*, and *Staphylococcus aureus* listed as critical and high priority pathogens, respectively [1]. The development of antibiotic resistance can occur naturally. However, mis- and overuse of antibiotics in the medical field and in agriculture are accelerating the process of antibiotic resistance build-up. Hence, growing numbers of bacterial infections with (multidrug) resistant bacterial strains have become a severe threat to humans worldwide [2,3]. Therefore, the design, investigation and production of new powerful antimicrobials are urgently needed [4,5]. Moreover, rapid sensing approaches to identify pathogens may help to ensure adequate precautions and targeted treatment in order to avoid the untargeted or even unnecessary administration of antibiotics. In particular, cost-effective, accurate, rapid and easy-to-use diagnostic devices that can be operated on-site as point-of-care systems are desirable, especially for use in remote areas without appropriate electricity or temperature control [6].

Standard microbiological detection methods are often time consuming, due to multi-step procedures, including cultivation for at least one day, staining or microscopic counting [7,8]. Molecular diagnostic techniques, often based on polymerase chain reaction (PCR) to amplify bacterial DNA in the sample, are considered to be rapid and

Peer review under responsibility of KeAi Communications Co., Ltd.
* Corresponding author.
E-mail address: schoenherr@chemie.uni-siegen.de (H. Schönherr).

https://doi.org/10.1016/j.bioactmat.2021.04.022
Received 28 December 2020; Received in revised form 12 March 2021; Accepted 9 April 2021

Abbreviation list

DMSO	Dimethyl sulfoxide
E. coli	*Escherichia coli*
EDC.HCL	*N*-(3-dimethylaminopropyl)-*N*-ethylcarbodiimide hydrochloride
EHEC	Enterohemorrhagic *Escherichia coli*
ESKAPE	*Enterococcus faecium, Staphylococcus aureus, Klebsiella pneumoniae, Acinetobacter baumannii, Pseudomonas aeruginosa,* and *Enterobacter* spp.
LB	Lysogeny broth
LOD	Limit of detection
LOQ	Limit of quantitation
MES	4-Morpholineethanesulfonic acid
Min	Minutes
Mod	Modification
mM	Millimoles per liter
MRSA	Methicillin-resistant *Staphylococcus aureus*
4-MU	4-Methylumbelliferone
MUD	4-Methylumbelliferyl α-D-glucopyranoside
NHS	*N*-Hydroxy succinimide
nM	Nanomoles per liter
4-NP	4-Nitrophenol
NSC	*N*-succinyl-chitosan
PBS	Phosphate-buffered saline
PCR	Polymerase chain reaction
PDA	Polydiacetylene
PDMS	Polydimethylsiloxane
PNPG	4-Nitrophenyl-β-D-glucuronide
S. aureus	*Staphylococcus aureus*
susp.	Suspension
w/V	Weight per volume
X-Gal	5-Bromo-4-chloro-3-indolyl-β-D-galactopyranoside
μL	Microliter
μM	Micromoles per liter
I_F	Fluorescence emission intensity

sensitive approaches, which allow the specific identification of certain pathogens. Apart from PCR, isothermal DNA-based recombinase polymerase amplification assays in a portable microfluidic cartridge diagnostic assay platform were recently applied for the detection of ESKAPE (*Enterococcus faecium, S. aureus, Klebsiella pneumoniae, Acinetobacter baumannii, Pseudomonas aeruginosa,* and *Enterobacter* spp.) bacterial species by Renner et al. [9]. However, the DNA based detection of bacteria requires qualified personnel and specific laboratory devices. Furthermore, it does not allow the differentiation between metabolically active and inactive bacteria [10].

More recently, reliable rapid detection and differentiation of bacterial species were realized with dedicated laboratory-based equipment, such as optical endomicroscopy [11], mass spectrometry [12,13], and a confocal laser scanning microscopy combined with white light laser technology [14]. These approaches, however, are usually complicated, expensive, and not suited for non-hospital settings.

Among the advanced alternative methods for bacterial infection sensing, nanomaterial-based approaches have received considerable attention. These approaches rely on e.g. nanoparticles [15–17], nanocapsules (liposomes and polymersomes) [18–21], nanopores or nanofibers [22–26], which specifically detect bacteria or bacterial infections. Additionally, bacteria detection or differentiation was also realized with either bacteria - targeting antibodies coupled to porous silicon [23], or "microrobots" [27], microfluidics, microarrays [28–30], nucleic acid-based molecular machines [31–33], as well as polymer or paper-based sensors [34–39]. For instance, liposomes and polymersomes as well as flexible bandages with integrated temperature and pH sensors have also been used for *S. aureus* detection [20,40,41], which is usually done by chromogenic differential culture medium as standard procedure [42]. In addition, nanofibers or micro-bio-electronic devices have been applied for *E. coli* detection [24,25,43] instead of standardized procedures [44–46].

As an alternative colorimetric sensing material, we have recently reported on colorimetric enzyme substrate-equipped chitosan films to detect bacteria in a fast and sensitive manner. This approach is based on the reaction of enzymes, produced and secreted by the target bacteria, with reporter units coupled to the chitosan films [47,48]. Furthermore, the concept was expanded to the detection and discrimination of various bacterial enzymes and bacteria exploiting various colors afforded by different substrates [49] or differently shaped patterns exhibiting the same [50] or different [51] colors.

S. aureus is a frequent cause of wound infections and consequently is one of the most common pathogens identified in clinical microbiology laboratories [52]. Highly resistant strains like the methicillin-resistant *S. aureus* (MRSA) are part of the so-called ESKAPE group, meaning bacterial pathogens of major concern for public health [53]. *S. aureus* can also provoke food poisoning [54] and produces various enzymes such as coagulase, hyaluronidase, deoxyribonuclease, lipase, staphylokinase, β-lactamase as well as other type of proteases [55,56]. Particularly, the exoglycosidase α-glucosidase is one of the identifier enzymes (ID marker) produced by *S. aureus,* which is used to discriminate *S. aureus* from other Staphylococci [52]. The enzyme hydrolyses terminal non-reducing (1->4)-linked α-D-glucose residues resulting in the release of α-D-glucose [49,52]. In addition, the absence of β-galactosidase activity can be used to differentiate *S. aureus* from other *Staphylococcus* species, such as *Staphylococcus intermedius*, *Staphylococcus pseudintermedius*, and *Staphylococcus schleiferi* subsp. *schleiferi,* according to the Manual of the Clinical Microbiology [57]. According to the same reference [57], no β-glucuronidase activity is detected for *S. aureus*.

E. coli O157:H7 is the most critical and well-studied EHEC serotype [58]. Transmission of EHEC occurs mainly through contaminated food. EHEC infections can lead to haemorrhagic colitis and haemolytic uremic syndrome. β-galactosidase and β-glucuronidase are common enzymes produced by *E. coli* strains, i.e. β-galactosidase is produced by more than 90% of *E. coli* strains including EHEC [59]. By contrast, most EHEC strains lack β-glucuronidase, although it is produced by more than 98% of *E. coli* strains, including the non-pathogenic strain *E. coli* DH5α [58,60,61]. *E. coli* DH5α, which is used in this study is a special strain since it produces β-glucuronidase, as mentioned, but *not* β-galactosidase due to mutations of the β-galactosidase gene (*lacZ*) [62]. Additionally, *E. coli* DH5α shows α-glucosidase activity [63], which is absent e.g. in *E. coli* O157:H7 EDL933 (EHEC) [64,65].

Standard chromogenic media exploit a substrate for β-glucuronidase to allow the specific identification of *E. coli* as the most common urinary pathogen. Due to the lack of β-glucuronidase among EHEC strains, media like CHROMagar O157 or Colorex™ O157 Agar allow the detection of EHEC among other *E. coli* [66]. Similarly, one may differentiate among different *E.* coli strains, e.g. certain EHEC and non EHEC *E. coli* strains, which was previously shown with an autonomously reporting chitosan hydrogel film sensor [67].

Here, we realized the multiplexed detection of bacterial enzymes and also directly of the bacterial strains producing them, in suspensions using three independent sensing moieties expanding our previously established concept of patterned sensing chitosan hydrogels [68]. The target enzymes liberate three readily distinguishable dyes in the sensor hydrogels (Fig. 1). By spatially separating the individual enzyme-reactive hydrogel spots and additionally encoding the functionality, i.e. the selectivity for a given enzyme by the color of the

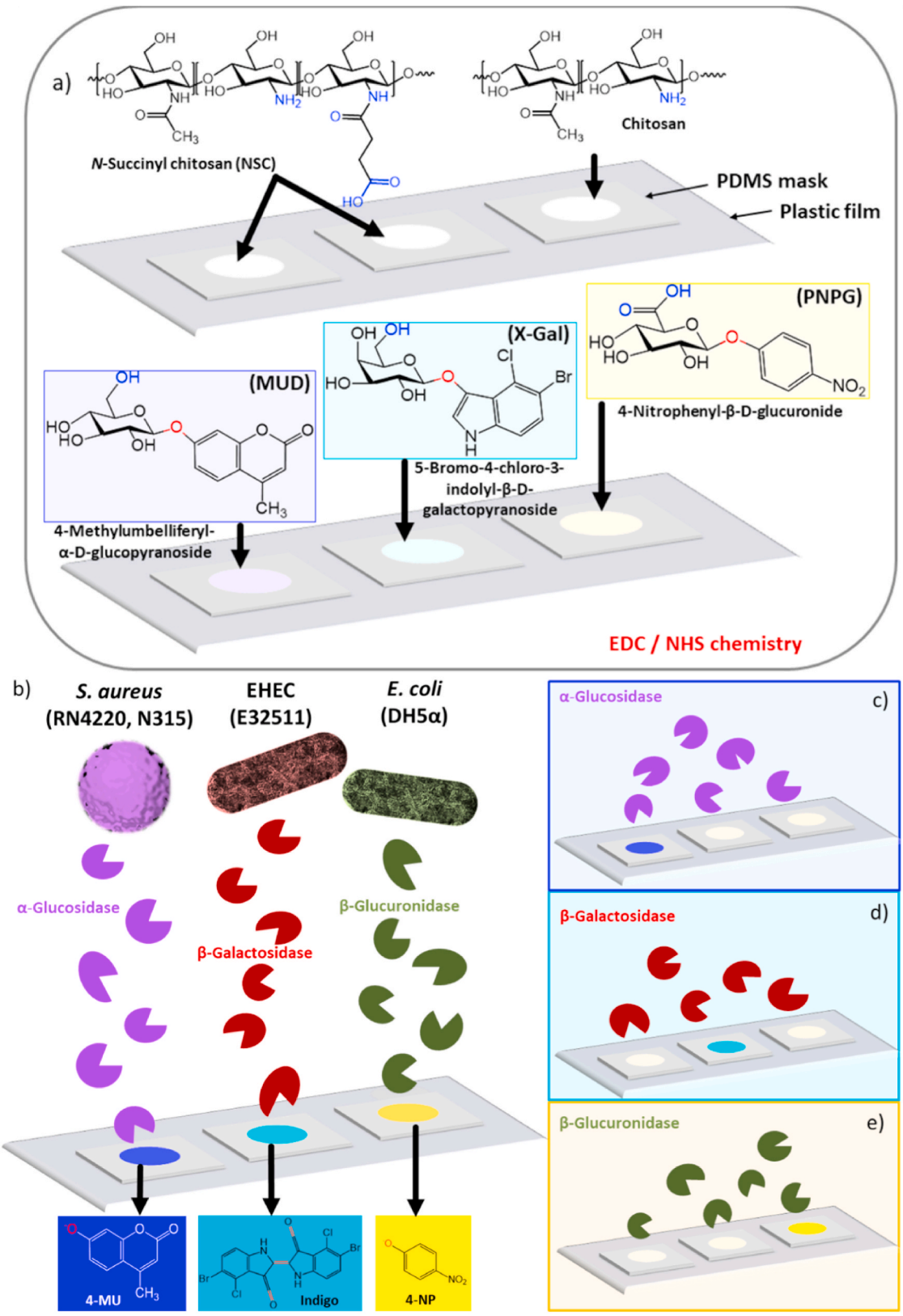

Fig. 1. Schematic of color-encoded sensor hydrogel for multiplexed bacterial enzyme differentiation and bacteria detection with the listed bacterial strains. a) Chemical structures of colorimetric substrates and hydrogel matrices as well as chemical modification of hydrogel in circular area with colorimetric substrates via *N*-(3-dimethylaminopropyl)-*N*-ethylcarbodiimide (EDC)/*N*-hydroxy succinimide (NHS) chemistry. b) The release of the dyes, which are characterized by different colors, is caused by cleavage reactions catalyzed by the corresponding target enzymes secreted from *S. aureus* RN4220, MRSA N315, EHEC E32511 and *E. coli* DH5α, respectively. c), d) and e) Schematic of release of specific dyes that occurs exclusively in presence of the target enzyme.

corresponding spot, the enzymes produced by diverse bacteria can be detected even by bare eye inspection in one glimpse under appropriate illumination. In this study, we have selected bacterial strains that differ in their enzyme profiles, as elucidated above, to assess the functionality of the system. In particular, we tested the multiplexed hydrogel system with strains of *S. aureus,* RN4220 and MRSA N315, and of *E. coli* DH5α and EHEC E32511, that can be discriminated by the combination of positive (released dye) and negative (no released dye) results from the three different hydrogels after the reaction with bacterial enzymes secreted by these individual bacterial strains.

2. Experimental

2.1. Materials

Silicon (100) wafers (P/Boron type, manufactured by OKMETIC, Finland), transparent films (Kopier-Folien CE 6088) and TC Plate 96-well (transparent and black, Sarstedt, Germany) were used as supporting substrates. Polydimethylsiloxane (PDMS) prepolymer and a curing agent (Sylgard 184) were purchased from Dow Corning (Germany). Chitosan (medium molar mass, 190–310 kDa, 75–85% deacetylated), 4-nitrophenyl-β-D-glucuronide (PNPG), 5-bromo-4-chloro-3-indolyl-β-D-galactopyranoside (X-Gal), succinic anhydride, *N*-(3-dimethylaminopropyl)-*N*-ethylcarbodiimide hydrochloride (EDC·HCl), *N*-hydroxy succinimide (NHS), 4-morpholineethanesulfonic acid (MES hydrate), α-glucosidase from *Saccharomyces cerevisiae* (16.13 units/mg protein, E. C. 3.2.1.20; type I), β-glucuronidase purified from *E. coli* (694.3 units/mg, E.C. 3.2.1.31; type IX-A), and β-galactosidase from *E. coli* (132.4 units/mg, E.C. 3.2.1.23), ethanol absolute, dimethyl sulfoxide (DMSO, 99%), 4-methylumbelliferone (4-MU) and 4-nitrophenol (4-NP) were purchased from Sigma-Aldrich (Germany). Acetone (99%, VWR, Germany), sodium hydroxide (98.8%, Chemsolute, Germany), 4-methylumbelliferyl-α-D-glucopyranoside (MUD, Roth, Germany), indigo (Roth) and acetic acid (glacial, J. T. Baker, Germany), Dulbecco's phosphate saline buffer (DPBS, 10 x, 95 mM (PO_4) without Mg^{2+} and Ca^{2+}, Lonza, Switzerland) were purchased from the listed suppliers. Milli-Q water was drawn from a Millipore Direct Q8 system with a resistivity 18.2 MΩ cm (Millipore advantage A10 system, Schwalbach, with Millimark Express 40 filter, Merck, Germany), phosphate saline buffer solution (PBS, pH 7.4) was prepared through the dilution of DPBS by Milli-Q water and volume ratio of DPBS and Milli-Q water was 1:9.

2.2. Bacteria

A series of four bacterial strains belonging to two different species were used in this study. Gram-positive bacteria used were *S. aureus* laboratory strain RN4220 [69,70] and MRSA N315 [71]. Gram-negative bacteria used were the laboratory strain *E. coli* DH5α [72] and EHEC E32511 [73]. The detailed information is provided in Table 1. All bacteria were cultured in Lysogeny broth (LB) at 37 °C.

2.3. Preparation of chitosan and N-succinyl-chitosan layers in 96-well plates

Chitosan layer preparation. Chitosan layers were prepared according to previously published work [68]. Aqueous chitosan solution (0.7% (w/v)) was prepared with 1 wt% acetic acid. Impurities and particles (d ≥ 2.5 μm) were removed by filtration (Whatman no. 5 qualitative filter paper). Chitosan solution (100 μL 0.7% (w/v)) was deposited into each well of a 96-well plate (transparent, polystyrene, flat bottom, Sarstedt, Germany). Afterwards, the samples were dried in a clean hood for 24 h, and subsequently neutralized with NaOH solution (100 μL, 0.1 M) for 1 min. Then, the chitosan layer was washed with copious amounts (100 μL each time, 3 times in total) of Milli-Q water. Finally, the samples were directly modified with the enzyme substrate PNPG.

Synthesis of N-succinyl-chitosan (NSC). NSC was prepared by ring-opening reaction using succinic anhydride in DMSO according to literature [74,75]. Chitosan (2.0 g) was added in 40 mL DMSO, which contained succinic anhydride (2.0 g). The reaction was carried out for 24 h at 60 °C with stirring. The mixture was filtered (Whatman no. 5 qualitative filter paper). The obtained solid was washed alternating by ethanol and acetone, and then dispersed into 100 mL Milli-Q water. The pH of the resulting suspension was adjusted to 10–12 by using NaOH solution (1 M). Afterwards, the clear suspension was filtered twice and reprecipitated in acetone. The final solid product was washed with ethanol followed by acetone and dried under vacuum at 50 °C.

NSC layer preparation. Aqueous NSC solution (100 μL 0.7% (w/v)) was deposited into each well of 96-well plates. The NSC layer was formed in 96-well plates after drying under fume hood for 24 h. The thickness of the NSC layer in each well was about 14 μm.

Table 1
Bacterial strains and inoculum concentrations used.

Strain	Origin/Characteristics	Inoculum applied (CFU/mL)
***Staphylococcus aureus* RN4220** [69,70]	ATCC 35556; laboratory strain generated through UV and chemical mutagenesis of *S. aureus* strain NCTC 8325-4; isolated from conjunctiva (corneal ulcer) in 1943; mutation in the *sau1 hsdR* gene	8×10^9
Methicillin-resistant *Staphylococcus aureus* (MRSA) N315 [71]	provided by the NARSA[a] for distribution via BEI Resources[b]; MRSA strain isolated from a pharyngeal smear of a Japanese patient in 1982	2×10^9
***Escherichia coli* DH5α** [72]	DSM No.:6897; derivative of strain K12 MM294 (*E. coli* (Migula 1895) Castellani and Chalmers 1919)	3×10^9
Enterohemorrhagic *Escherichia coli* (EHEC) E32511 [73]	Isolated from a patient with haemolytic uremic syndrome (HUS), England, 1983; serotype O157:H7 (EHEC)	6×10^8 (susp. 1) 9×10^8 (susp. 2)

[a] NARSA: Network on Antimicrobial Resistance in *Staphylococcus aureus*.
[b] BEI Resources: Biodefense and Emerging Infections Research Resources Repository, access via the National Institute of Allergy and Infectious Diseases [NIAID] as part of the National Institute of Health (NIH).

2.4. Modification of chitosan/NSC with enzyme substrates

Grafting of PNPG to chitosan hydrogels in 96-well plates. PNPG (10 mM) was prepared in PBS (pH 7.4) at ambient atmosphere, followed by addition of EDC·HCl (3 mol/mol of PNPG) and NHS (3 mol/mol of PNPG). Then, the solution was stirred for 1 h. One hundred μL of the modification solution was added to each well, which contained neutralized chitosan layers. The modification was performed for 6 h under shaking (rate: 60 Hz) at ambient condition. The modified chitosan layer in each well was exhaustively washed under shaking (60 Hz, Milli-Q water replacement intervals of 30 min) for 2 h after thoroughly rinsing in 100 μL Milli-Q water using pipetting and then dried under fume hood for a night. The β-glucuronidase sensing hydrogels showed typical degrees of swelling of 300% as determined by gravimetry. Dry films were directly used for enzymatic reaction in a not pre-swollen state.

Grafting of MUD/X-Gal to NSC hydrogels in 96-well plates. X-Gal (2.5 mM) or MUD (2.5 mM) was dissolved in a mixed solution of DMSO and buffered MES solution (pH 5.5), with a volume ratio of 1:4. Mixed solutions of EDC (30 mM) and NHS (30 mM) were prepared in buffered MES solution (pH 5.5). One hundred μL of mixed solutions of EDC/NHS was added to each well, which contained the NSC layer, and the activation reaction was carried out for 1.5 h under shaking (rate: 60 Hz) at ambient condition. Afterwards, 100 μL of X-Gal/MUD solution was added to the wells, which contained the active hydrogel by EDC/NSC

solution. The modification was performed for 6 h under shaking (rate: 60 Hz) at ambient conditions after removing the reacted EDC/NHS solution from each well in 96-well plates. Finally, the solution in the wells was sucked out and followed by rinsing with Milli-Q water and drying under a laminar flow hood overnight. Dry films were directly used for enzymatic reaction in a not pre-swollen state.

Grafting of MUD to NSC film on silicon substrate. Aqueous NSC solution (108 μL, 2.1% (w/v)) was deposited on a cleaned silicon wafer (cleaned with an UV- Ozone cleaner, ProCleaner TM system, supplied by Bioforce Nanosciences, 30 min). Afterwards, the samples were dried under clean hood for 24 h. The dried NSC film was activated by immersing in 2 mL of a mixed solution of EDC (30 mM) and NHS (30 mM) in buffered MES (pH 5.5) for 1.5 h under shaking (60 Hz) at ambient conditions. Then, the activated NSC film was transferred into 2 mL of MUD solution (2.5 mM, mixed solvents of DMSO and buffered MES solution (pH 5.5) with a volume ratio of 1:4) and immersed for 6 h under shaking (60 Hz) at ambient conditions, followed by rinsing with Milli-Q water and drying in a laminar flow hood overnight. Dry films were directly used for enzymatic reaction in a not pre-swollen state.

2.5. Preparation of patterned samples

PDMS mask preparation. A PDMS mask was prepared according to the literature [76]. The PDMS prepolymer and curing agent (Sylgard 184) were mixed in a 10:1 ratio (by weight) and poured into a polystyrene petri dish after 30 min of degassing. The curing process was performed in an oven at 70 °C for 1 h. Circular (⌀ = 6 mm) holes were drill pierced after the cured PDMS had cooled to ambient temperatures (thickness 2.8 mm).

Substrate modification on embossed chitosan patterns. A cleaned transparent plastic film (2.6 × 7.6 cm^2) was covered with the PDMS masks, which possessed 15 circular-shaped (⌀ = 6 mm) holes in three parallel columns. NSC solution (100 μL, 0.7% (w/v)) was deposited into each well on the first two columns and chitosan solution (100 μL, 0.7% (w/v)) was deposited into each well on the last column. The entire film was dried in a clean hood for 24 h. The chitosan film in the last column was neutralized by NaOH solution (0.1 M, 100 μL) for 1 min and rinsed with Milli-Q water. One hundred μL of mixed solution of EDC (30 mM) and NHS (30 mM) were added to each well, which contained NSC layers in the first two columns. The activation process was carried out for 1.5 h under shaking (rate: 60 Hz) at ambient condition. After removing the reacted EDC/NHS solution from each well, 100 μL of MUD (2.5 mM) and X-Gal (2.5 mM) solution was added to the wells, which contained the active hydrogel on the 1st and 2nd column, respectively. In the meantime, 100 μL of PNPG modification solution (10 mM) after 1 h reaction with EDC (30 mM)/NHS (30 mM) were added to each well in the 3rd column. All the modification processes between enzyme substrates and chitosan/NSC layer were performed for 6 h under shaking (rate: 60 Hz) at ambient conditions. Final washing steps were performed as described for the 96-well plates before and the samples were dried in a laminar flow hood overnight. All dry hydrogels were directly used for enzymatic reaction in a not pre-swollen state.

2.6. Enzymatic reactions

Enzymatic reactions in the hydrogels in 96-well plates. Buffered enzyme solution (100 μL, PBS, pH 7.4) with varied concentrations was added into each well, which contained the grafted chitosan/NSC samples. The plate was immediately covered with a transparent foil and measured using a microplate reader. The details of the measurement parameter are mentioned in the captions of corresponding results (Fig. 2c–f and S3-5).

Enzymatic reactions in the hydrogels on silicon substrate. One piece of α-glucosidase sensing hydrogel on a silicon substrate was inserted into 1 mm path-length quartz cell. The quartz cell was closed with Parafilm after the addition of buffered α-glucosidase enzyme solution (0.2 μM, 150 μL, PBS, pH 7.4). The fluorescence spectra were recorded in a spectrometer immediately. The details of the measurement parameter are mentioned in the captions of corresponding results (Fig. 2a and b).

Enzymatic reactions in the patterned hydrogels. Buffered enzyme solution (mixture of 100 μL of 0.6 μM α-glucosidase, 100 μL of 0.6 μM β-galactosidase and 100 μL of 0.6 μM β-glucuronidase, in PBS, pH 7.4, 70 μL in each pattern) was dropped on the 2nd row. Individual buffered enzyme solution (PBS, pH 7.4) of α-glucosidase (0.2 μM, 70 μL on each pattern), β-galactosidase (0.2 μM, 70 μL on each pattern) and β-glucuronidase (0.2 μM, 70 μL on each pattern) were dropped into each well of the 3rd to 5th rows, respectively. As the blank, PBS was added into each well of the 1st row. The color changes on the patterned areas during the enzymatic reaction were recorded by an iSight camera under white light illumination in front of a white background or UV illumination by a hand-held standard UV lamp in front of a black background.

2.7. Fluorescence spectroscopy

Measurements were carried out either with a Varian Cary Eclipse spectrometer (Mulgrave, Victoria, Australia) or with microplate readers (Tecan SAFIRE, Tecan, Switzerland or LB 943 Mithras^2, Berthold, Germany) at 25 °C. Fluorescence spectra obtained with the Varian Cary Eclipse spectrometer were measured at a scan rate of 120 nm/min and a resolution of 5 nm for the excitation and emission, using a 1 mm path-length quartz cell (SUPRASIL, Hellma Analytics, Germany). Fluorescence intensity measurements, which were recorded on the microplate reader, were performed using 96-well plates (black, polystyrene, flat bottom, Sarstedt, Germany) as sample holder with clear viewseal sealer (Greiner Bio-One, Austria). A bandwidth of 12 nm was applied for both excitation and emission. The gain parameter was manually set to 70 for the Tecan SAFIRE and to 255 for the LB 943 Mithras^2, respectively.

2.8. UV–visible spectroscopy

Measurements were carried out on several microplate readers (Tecan SAFIRE, Tecan, Switzerland; LB 943 Mithras^2, Berthold, Germany; Synergy H1, BioTek, United States) at 25 °C. UV–vis spectra were recorded using a 96-well plate (transparent, polystyrene, flat bottom, Sarstedt, Germany) as sample holder with clear viewseal sealer (Greiner Bio-One, Austria). The spectra were obtained in the wavelength range from 340 nm to 500 nm or 800 nm for the hydrogels that release 4-nitrophenol or 5,5′dibromo-4,4′-dichloro-indigo, respectively. A 1 nm wavelength step size was using for the Tecan SAFIRE for enzyme detection and the LB 943 Mithras^2 performing the *E. coli* DH5α strain detection, and a 2 nm was used for the Synergy H1 for the EHEC strain detection, respectively.

2.9. Attenuated total internal reflection-fourier transform infrared (ATR-FTIR) spectroscopy

ATR-FTIR analysis was carried out using a Tensor 27 FTIR spectrometer (Bruker Optik GmbH, Ettlingen, Germany). The hydrogel (Chitosan, NSC, Enzyme sensing hydrogels) on silicon substrate was placed and fixed in the chamber of the instrument. The measurements were performed in absorbance mode in the spectral range 4000 to 600 cm^{-1} and a spectral resolution of 4 cm^{-1}. The background spectra were obtained by using air.

2.10. Determination of the limit of detection (LOD) and limit of quantitation (LOQ)

The values of the LOD for the detection of the reporter dyes as well as for the enzymes using microplate readers were determined according to the literature [47]. The details of the determination of the LOD values for the detection of the dyes (Figure S6) and for the enzymes by bare eye detection and in the microplate reader, including the LOQ values (Figure S7), are described in the Supporting Information.

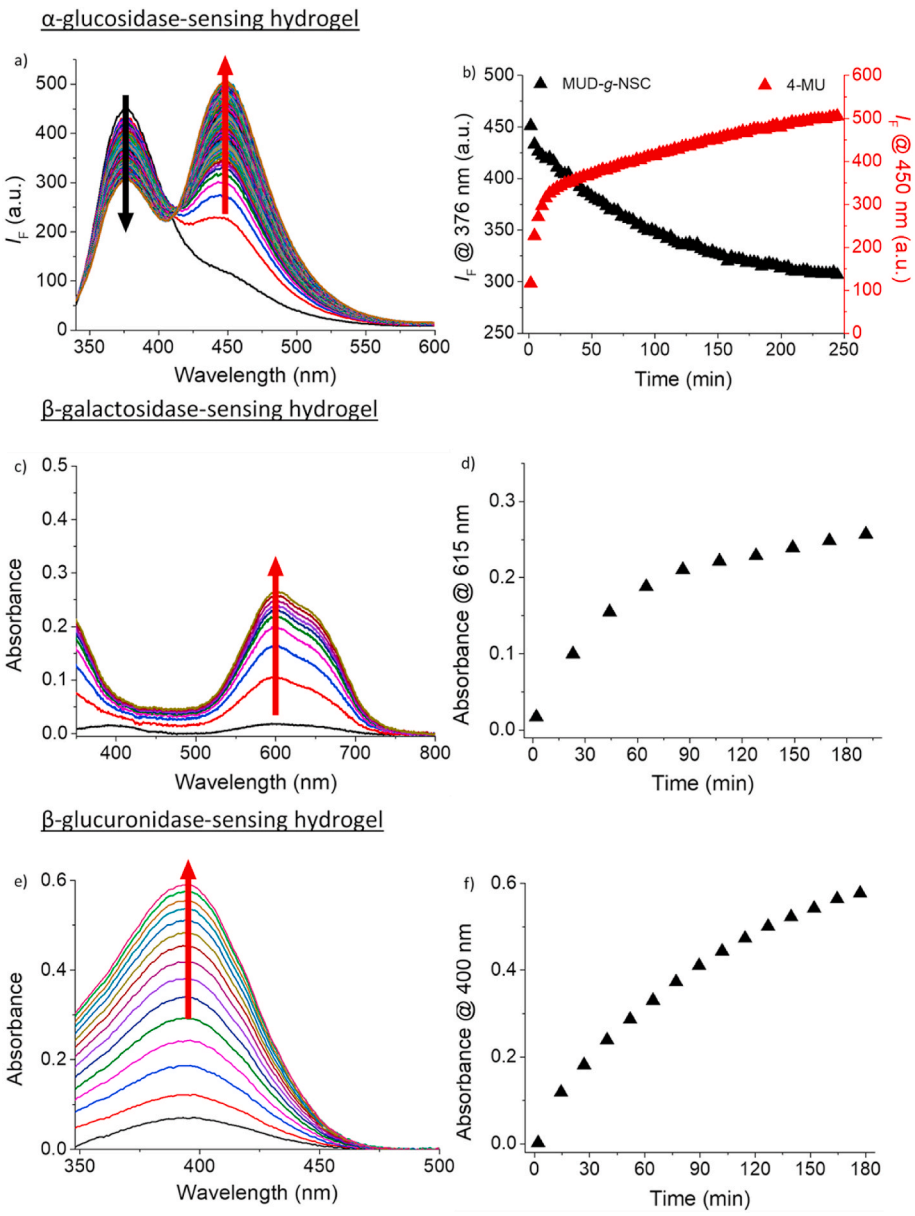

Fig. 2. a) Fluorescence spectra (measured in a fluorescence spectrometer) of 4-MU released during the enzymatic reaction in α-glucosidase sensing hydrogel (MUD-*g*-NSC) on silicon. ($[MUD]_{mod}$ = 2.5 mM; [α-Glucosidase] = 0.2 μM, λ_{ex} = 325 nm, measurement repeat interval: 3 min). b) Plot of I_F at λ_{max} = 376 nm of MUD and at λ_{max} = 450 nm of 4-MU in panel a) versus time. c) UV–vis spectra (microplate reader) of dimerized indigo during the enzymatic reaction in the β-galactosidase sensing hydrogels in a transparent 96-well plate ($[X\text{-}Gal]_{mod}$ = 2.5 mM, [β-Galactosidase] = 0.2 μM, measurement repeat interval: 21 min). d) Plot of absorbance at λ_{max} = 615 nm of dimerized indigo in panel c) versus time. e) UV–vis spectra (microplate reader) of released 4-NP during the enzymatic reaction in the β-glucuronidase sensing hydrogels in a transparent 96-well plate ($[PNPG]_{mod}$ = 10 mM; [β-Glucuronidase] = 0.2 μM, measurement repeat interval: 12.5 min). f) Plot of absorbance at λ_{max} = 400 nm of released 4-NP in panel e) versus time. The arrows indicate the temporal changes in the spectra.

2.11. Bacterial culture and detection

One single colony from agar plates of each bacterial strain was transferred to a 15 mL reaction tube containing 5 mL LB, where it was incubated at 37 °C and 200 rpm for 16 h. For the *E. coli* strains, the optical density (OD) of the suspensions was obtained by measuring the absorbance at λ = 650 nm (OD_{650}) using a path length of 1 cm. Afterwards, the suspension was diluted to OD_{650} = 0.8 with fresh LB. These bacterial suspensions were then 100-fold (EHEC E32511) or 1000-fold (*E. coli* DH5α) diluted with LB and were incubated for 24 h (*E. coli* DH5α) or for 24 h and 48 h (EHEC E32511) at 37 °C and 200 rpm. Finally, 100 μL of the resulting sub-cultured *E. coli* DH5α and EHEC E32511 suspensions as well as the 16 h cultured *S. aureus* RN4220 and MRSA N315 bacterial suspensions were added to 96-well plates, which contained α-glucosidase, β-glucuronidase, or β-galactosidase sensing hydrogel samples for further measurements (n = 3, biotriplicates, kinetics or spectral measurements with a microplate reader). LB was added into 96-well plates, which contained the enzyme sensing hydrogel samples as blank experiment. The bacterial suspensions in empty wells in the 96-well plates were used for background calibration. Additionally, the suspensions were serially diluted, plated onto LB or blood agar plates and incubated at 37 °C overnight to determine the number of colony forming units (CFU)/mL of the corresponding inoculum.

3. Results and discussion

The rationale of the color-encoded patterned sensor hydrogels for the rapid, sensitive, selective and multiplexed detection and differentiation of the three different bacterial enzymes, as well as the corresponding detection of living and thus metabolically active bacteria, are shown schematically in Fig. 1. Three different colorimetric substrates were grafted to chitosan or NSC hydrogels, which were patterned onto a neat soft plastic film. In this configuration (i.e. when the hydrogel is in its native state), no color was detected. By contrast, after the corresponding selective enzymatic reactions with the target enzymes, i.e. α-glucosidase, β-galactosidase and β-glucuronidase that are differentially produced by the test strains of *S. aureus* RN4220, MRSA N315, *E. coli* DH5α and EHEC E32511, three different dyes were released from the enzyme sensing hydrogels (Fig. 1b).

Chitosan hydrogels were modified with the chromogenic substrate

PNPG by EDC/NHS chemistry via robust amide bond formation between the carboxyl groups in the enzyme substrate and the amine groups in chitosan. For the synthesis of α-glucosidase and β-galactosidase sensing hydrogels, NSC was synthesized by modification of chitosan powder with succinic anhydride in a ring-opening reaction in a first step [74]. Afterwards, the NSC hydrogels were activated by EDC/NHS and subsequently functionalized with the fluorogenic substrate MUD or the chromogenic substrate X-Gal via formation of an ester bond.

Due to the enzymatic cleavage of labile bonds in the substrates inside the hydrogels, 4-MU, 5,5′dibromo-4,4′-dichloro-indigo as blue water-insoluble indigo dye, formed from the initially released indole derivative by dimerization in the presence of oxygen, and 4-NP were formed and could be detected during the corresponding enzymatic reactions. All the details of hydrogel synthesis and enzymatic reactions are shown in Figure S1. The modification was confirmed by FTIR spectroscopy. In the FTIR spectra (Figure S2a) of β-glucuronidase-sensing hydrogel, the band at 1585 cm^{-1} (attributed to the primary amine of the glucosamine unit of chitosan) disappeared, whereas the bands at 1645 and 1551 cm^{-1} became stronger, which are attributed to the amide I and II vibrations, respectively. This observation is consistent with the formation of new amide bonds in the β-glucuronidase-sensing hydrogel. In the FTIR spectra (Figure S2b) of α-glucosidase-sensing hydrogel and β-galactosidase sensing hydrogel, two bands at 1182 and 1153 cm^{-1} (C-O stretching in ester bond) appeared, which are attributed to the ester bond. These indicate the ester bond formation after modification of enzyme substrate with NSC. Combined with highly reproducible dye released process during the enzymatic reaction of the hydrogels in Figure S3 and Figure S4, it is confirmed that MUD and X-Gal enzyme substrates were successfully grafted to NSC. Furthermore, according to the enzymatic reaction kinetics at the plateau phase (Figure S3-5a) as well as the calibration curve of the released dye (Figure S6), the loading of enzyme substrate in enzyme sensing hydrogel (each piece of hydrogel in a well of 96 well-plates) was obtained, i.e. about 2.9 μg of MUD substrate in *N*-succinyl-chitosan (7 mg), 4.0 μg of X-Gal substrate in *N*-succinyl-chitosan (7 mg) and 0.7 μg of PNPG substrate in chitosan (7 mg).

3.1. Enzymatic reactions in enzyme sensing hydrogels

The enzymatic reactions of the investigated α-glucosidase, β-glucuronidase and β-galactosidase sensing hydrogels were first performed in aqueous buffered enzyme solution (PBS, pH 7.4). The fluorescence spectra acquired during the enzymatic reaction in the α-glucosidase sensing hydrogel on a silicon wafer are shown in Fig. 2. The data were recorded in front face illumination in a fluorescence spectrometer. UV–vis spectra obtained during the enzymatic reactions in β-galactosidase and β-glucuronidase sensing hydrogels were performed in a 96-well plate format in a microplate reader.

Enzymatic reactions in α-glucosidase sensing hydrogels. The coumarin derivative 4-MU was liberated after the addition of α-glucosidase by the enzymatic cleavage of the fluorogenic substrate MUD conjugated to the NSC hydrogel, as can be seen in Fig. 2a. The changes in fluorescence emission detected in Fig. 2a are due to the formation of the deprotonated dye in the hydrogel. The deprotonated free 4-MU and the MUD conjugated to the hydrogel can thus be differentiated by fluorescence spectroscopy. When excited at a wavelength λ_{ex} of 325 nm, the emissions of 4-MU and MUD were centered at λ_{em} = 450 nm [77] and 376 nm, respectively, in buffered enzyme solution (pH 7.4). By adding 0.2 μM buffered α-glucosidase solution (PBS, pH 7.4), the I_F at about 450 nm increased monotonically due to the formation of free deprotonated 4-MU during the reaction. Consequently, the emission at about 376 nm decreased as a function of time, because of the consumption of the MUD in the hydrogel (Fig. 2b). The initial apparent rate for the formation of 4-MU was found to be 28 (±4) min^{-1} in the first 15 min of the enzymatic reaction in the hydrogel. Compared to the method reported by Ebrahimi et al. before [49], the rate observed here was significantly higher, even at 800 times lower enzyme concentration. This is likely caused by the enhanced fraction of MUD substrate grafted to the hydrogel, which is accessible for the enzymes. By comparing the maximum fluorescence intensity, which is attributed to MUD, in both reports, one may conclude that the loading of MUD substrate in the hydrogel was presumably 3 times higher in this current work compared to the previously published work [49]. On the one hand, in the present work, NSC on silicon wafer was obtained by deposition of pre-synthesized NSC solution rather than by performing a ring opening reaction on the chitosan layer in succinic anhydride solution. Not surprisingly, it is more efficient to synthesize NSC in bulk solution. In addition, the EDC/NHS reaction [78] under acidic conditions, such as MES buffer, which was applied in this work to graft the enzyme substrate to the hydrogel, is more efficient than in phosphate buffer at neutral pH conditions, as used by Ebrahimi et al. [49]. Besides, an increased concentration of enzyme substrate in the modification reaction leads to an increased degree of functionalization of the hydrogel [49]. Thus, the higher reaction rate might be caused by 1) a significantly increased amount of MUD inside of the α-glucosidase sensing hydrogel and 2) a presumably more open network structure that facilitates enzymatic attack.

The kinetics of the enzymatic reaction in the hydrogel in a microwell plate format with various concentrations of α-glucosidase was recorded by sequential I_F measurements at λ_{max} = 450 nm (λ_{ex} = 365 nm) (n = 3). Plots of I_F versus time are shown in Figure S3a. The initial apparent reaction rate (t ≤ 15 min) was found to depend linearly on the initial enzyme concentration, with an apparent rate constant of 1766 (±94) $min^{-1}\mu M^{-1}$ (Figure S3b). The apparent rate constant is defined as the slope of the plot of initial apparent reaction rate over the initial enzyme concentration (Figure S2b) and was obtained using a linear least squares fit of the plot. In addition, to prove that the released 4-MU was formed due to a selective enzymatic cleavage of the C−O bond in the enzyme sensing hydrogel only by α-glucosidase, blank experiments in PBS and negative controls with solutions of different enzymes, i.e. β-galactosidase and β-glucuronidase, were carried out. In these controls, I_F remained constant (Figure S3c, d). Therefore, the α-glucosidase sensing hydrogel can be utilized for the selective detection of α-glucosidase and discriminate this enzyme from β-galactosidase and β-glucuronidase.

Enzymatic reactions in β-galactosidase sensing hydrogels. The enzymatic reaction of the β-galactosidase sensing hydrogel was performed in aqueous buffered enzyme solution (PBS, pH 7.4). The labile bond of the chromogenic substrate X-Gal was cleaved by β-galactosidase and after dimerization a water-insoluble blue indigo dye was formed inside the hydrogel. In Fig. 2c, the increasing absorbance in the wavelength ranging from 550 nm to 700 nm is associated with the formation of the dimerized indigo derivative during the enzymatic reaction of the hydrogel after the addition of 0.2 μM β-galactosidase solution. A monotonic increase of absorbance at λ_{max} = 615 nm was observed with increasing reaction time (Fig. 2d). Additionally, by recording the kinetics of the enzymatic reaction in the hydrogel with various concentrations of β-galactosidase (Figure S4a), it was found that the initial apparent reaction rate (for $t \leq 20$ min) depended linearly on the initial enzyme concentration (Figure S4b). The apparent rate constant was equal to 0.033 (±0.003) $min^{-1}\mu M^{-1}$ here, which is 10-fold larger than in our previous work [50]. This difference is likely due to the increased loading with X-Gal substrate in the hydrogel, as well as enhanced hydrogel swelling. As expected, PBS and buffered solutions of α-glucosidase and β-glucuronidase did not cause any significant changes of the absorbance at 615 nm (Figure S4c, d). Thus, the results confirmed that the dimerized indigo was formed due to the selective enzymatic cleavage of the C−O bond in the sensing hydrogel by β-galactosidase.

Enzymatic reactions in β-glucuronidase sensing hydrogels. The enzymatic reaction of the β-glucuronidase sensing hydrogel was performed in aqueous buffered enzyme solution (PBS, pH 7.4). The 4-NP was released from the glucuronide after adding β-glucuronidase. The corresponding UV–vis spectra are plotted in Fig. 2e. The monotonously increasing absorbance at about 400 nm is associated with the formation of 4-NP

during the reaction (Fig. 2f). Moreover, the kinetics of the enzymatic reaction in the hydrogel with various concentrations of β-glucuronidase was recorded, as shown in Figure S5a. With increasing initial enzyme concentration, the initial apparent reaction rate (t ≤ 30 min) showed a linear increase (Figure S4b). The apparent rate constant was equal to 0.034 (±0.002) $min^{-1}\mu M^{-1}$, which is slightly higher than the one reported before in the literature [47], likely due to the higher PNPG loading as a consequence of the higher concentration of PNPG in the modification solution. No change in the absorbance at 400 nm was observed during the reaction of the hydrogel with α-glucosidase and β-galactosidase, nor in the neat PBS (Figure S5c, d). Accordingly, the yellow 4-NP was only detected in the presence of β-glucuronidase, but not with α-glucosidase and β-galactosidase.

3.2. Determination of the limit of detection

The limit of detection (LOD) for the detection of the enzymes in the three enzyme sensing hydrogels is defined as the lowest concentration of the corresponding enzyme that can be detected by producing the released reporter dye at a concentration of the LOD of this dye. The LOD and LOQ are defined as background plus three and plus ten times the standard deviation of the background, respectively [79]. Hence, the LOD and LOQ for the detection of each enzyme depend not only on the instrument or the detection method, but also on the observation time [48]. To estimate the LOD values for the detection of the enzymes, the LOD and LOQ of the released dye were first determined according to previously published procedures [47]. The LOD of the enzyme was estimated using I_F or the absorbance corresponding to the LOD of the dye divided by the value of the rate constant (the slope of the plot for the initial reaction rate versus enzyme concentration, in Figure S3-5b) multiplied with the observation time. The corresponding plots of LOD for α-glucosidase, β-galactosidase and β-glucuronidase versus time determined in measurements in the microplate reader are shown in Fig. 3 and those determined for bare eye detection (Figure S8) are shown in Figure S9. In comparison to earlier studies, which utilized more sensitive fluorescence or UV–vis spectrometers, the LOD values of α-glucosidase and β-glucuronidase sensing hydrogel reported here, are improved by a factor of 100 [49] and 3 times [47], respectively. The LOD of β-galactosidase sensing hydrogel obtained here is similar to the one reported in the literature (≤3 nM) [50]. The details are shown in Table S1. Additionally, the values for the LOD for the detection of the enzymes at an observation time of 60 min are much lower than the enzyme concentrations in overnight cultured bacteria suspension, which are about 7–85 μM of α-glucosidase in *S. aureus* [49], 60 nM of β-glucuronidase in *E. coli* [61], and about 7 nM of β-galactosidase in EHEC [67].

The LODs for bare eye detection of the dyes in solution were determined by a blinded experiment. The results are summarized in Table S2 according to data from Figure S8. As expected, much lower LOD values were obtained when using a microplate reader, as compared to bare eye detection. The LODs for bare eye detection of 4-MU, indigo, and 4-NP solution were 10–100 times higher than with a microplate reader, corresponding to 10 μM, 8 μM and 20 μM, respectively. It should be mentioned that an improved detection with the help of mobile phone or related type devices was shown to be feasible [80].

3.3. Enzymatic reactions in patterned enzyme sensing hydrogels

To highlight the possibility to exploit the sensor hydrogels in a multiplexed fashion, patterned enzyme sensing hydrogels were applied for the rapid detection and discrimination of specific enzymes produced by the test strains of *S. aureus* RN4220, MRSA N315, *E. coli* DH5α and EHEC E32511.

In Fig. 4, patterned α-glucosidase, β-galactosidase, and β-glucuronidase sensing hydrogels were formed in the wells defined by PDMS in the 1st, 2nd and 3rd rows, respectively. Seventy μL of the mixed buffered enzyme solution were applied to three individual wells in the 2nd row, which contained enzyme sensing hydrogels. Individual enzymes, i.e. α-glucosidase (0.2 μM), β-galactosidase (0.2 μM) and β-glucuronidase (0.2 μM), were applied to each well in the 3rd to 5th rows, respectively. The enzymatic activities of the three different enzyme sensing hydrogel patterns according to the signals illustrated in Fig. 4 are summarized in Table 2. After 110 min, intense colors were observed in the patterned area containing enzyme sensing hydrogels under appropriate illumination, exclusively when the relevant enzyme was present ('+' in Table 2 means that the particular color was visible). According to the corresponding kinetics (Figure S3-5a), the enzymatic reactions of the hydrogels in 96 well-plate reached the plateau at this time. Additionally, based on the results of the LOD of dye by bare eye detection, the enzyme sensing hydrogels can be used to signal the bacterial enzyme under tested condition in less than 10 min, i.e. 3 min for α-glucosidase, 9 min for β-galactosidase and β-glucuronidase.

Specifically, a strong fluorescence signal from the released fluorophore 4-MU could be detected in the 2nd and 3rd rows of the first column after exposition to α-glucosidase containing solutions. Blue color from the dimerized indigo was visible only in the 2nd and 4th rows in the 2nd column and the yellow color from the released 4-NP was visible in the 2nd and 5th rows in the 3rd column after exposition to β-galactosidase and β-glucuronidase containing solutions, respectively. Consistently, PBS, added as a blank to each well in the 1st row, showed colorless patterns.

Additionally, independent spectroscopic measurements confirmed that the two unrelated enzymes in each case of the three hydrogels tested here could not break the bond in the enzyme substrates and did not produce any signal visible by bare eye under appropriate illumination or in changes in the spectra as observed in spectroscopic measurements (Figure S3-5c).

In summary, the patterned enzyme sensing hydrogels can indeed be

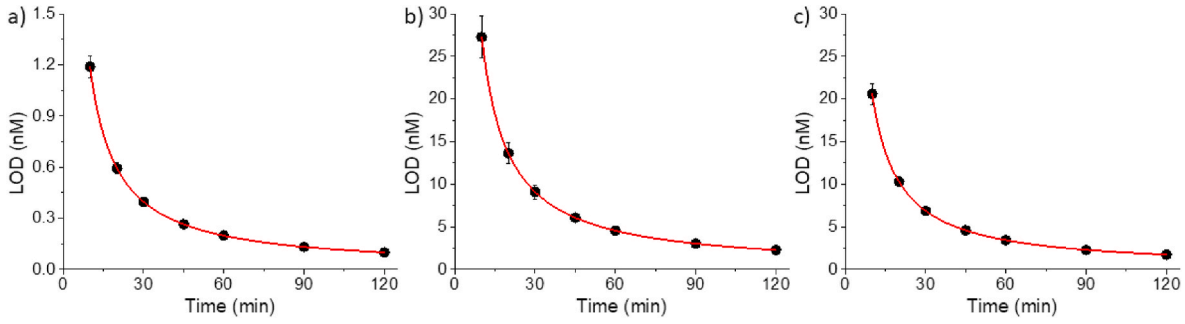

Fig. 3. Plots of the LOD versus time estimated for a) α-glucosidase in α-glucosidase sensing hydrogel, b) β-galactosidase in β-galactosidase-sensing hydrogel, and c) β-glucuronidase in β-glucuronidase-sensing hydrogel (microplate reader, 96-well plate, $[MUD]_{mod}$ = 2.5 mM, $[X\text{-}Gal]_{mod}$ = 2.5 mM, $[PNPG]_{mod}$ = 10 mM, 25 °C). The data were fitted with: a) LOD $_{(\alpha\text{-glucosidase})}$ = 11.9 nM min t^{-1}; b) LOD $_{(\beta\text{-galactosidase})}$ = 272.7 nM min t^{-1}; c) LOD $_{(\beta\text{-glucuronidase})}$ = 205.9 nM min t^{-1} (error bars: standard deviation, n = 3).

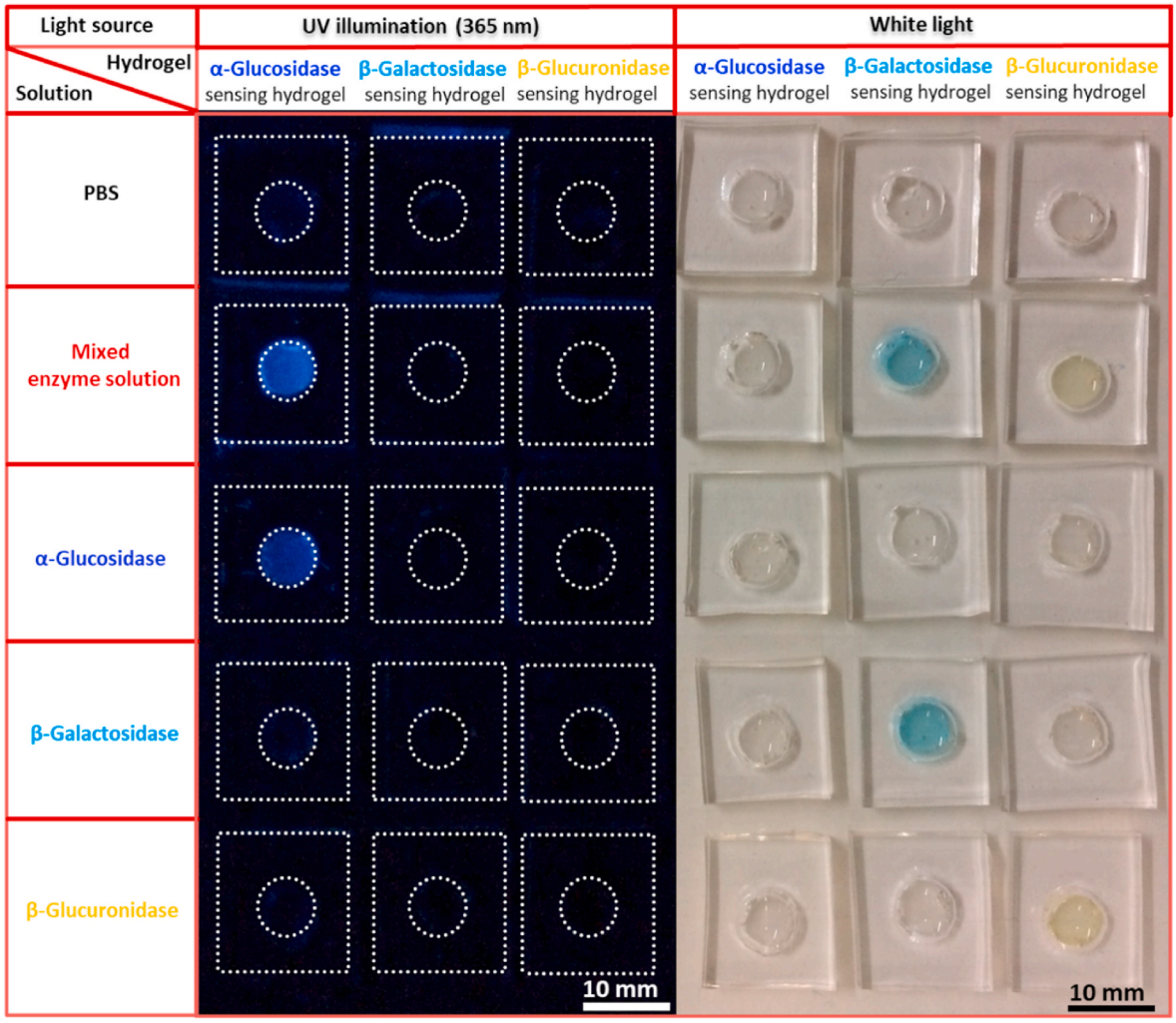

Fig. 4. Photograph of the color-encoded enzyme sensing hydrogels after enzymatic reactions. The photo was taken after a reaction time of 110 min at 25 °C, under UV illumination (hand-held lamp, λ_{ex} = 365 nm, left) on a black background as well as white light (right) on a white background. Circularly patterned chitosan was modified with MUD, X-Gal or PNPG substrates with the help of PDMS mask. ($[MUD]_{mod}$ = 2.5 mM, $[X\text{-}Gal]_{mod}$ = 2.5 mM, $[PNPG]_{mod}$ = 10 mM). PBS was added in the 1st row. A mixed enzyme solution (final concentration of each enzyme is corresponding to 0.2 μM) was applied in each pattern in the 2nd row. Individual solutions of α-Glucosidase, β-Galactosidase and β-Glucuronidase (all 0.2 μM) were added in the 3rd to 5th row, respectively (the length and thickness of the square PDMS mask are about 16 mm and 2.8 mm, respectively; 70 μL of the enzyme solution was applied into each circular area).

Table 2
Enzymatic activity in three different enzyme sensing hydrogel patterns.

Added solutions	Hydrogel type		
	α-glucosidase sensing hydrogel	β-galactosidase sensing hydrogel	β-glucuronidase sensing hydrogel
PBS (pH 7.4)	–	–	–
mixture[a]	+	+	+
α-glucosidase	+	–	–
β-galactosidase	–	+	–
β-glucuronidase	–	–	+

+: active (color change in the hydrogel pattern).
–: inactive (no color change in the hydrogel pattern).
[a] Mixed enzyme solution contains α-glucosidase, β-galactosidase, β-glucuronidase.

used for the bacterial enzyme detection and for differentiation among α-glucosidase, β-galactosidase and β-glucuronidase by bare eye detection in a multiplexed format.

3.4. Enzymatic reactions of enzyme sensing hydrogels in bacterial suspensions

As a further critical step to demonstrate the functionality of the sensor hydrogels, they were applied to detect and distinguish selected clinically relevant bacterial test strains based on their characteristic enzyme expression profile (Table 3). This evaluation with viable bacteria was performed by adding bacterial suspensions to the hydrogels. The diagnosis of EHEC, as one of the most problematic and pathogenic group among *E. coli* strains, is difficult, since there is no unique specifically expressed enzyme, which can discriminate EHEC from other *E. coli* strains. As a first step towards an enzyme-based detection system, we investigated a combined detection of β-galactosidase and β-glucuronidase, which are produced by most *E. coli* strains. β-galactosidase is indeed produced by >90% [60] and β-glucuronidase is expressed by more than 98% of *E. coli* strains, including *E. coli* DH5α. By contrast most EHEC strains, however, lack β-glucuronidase [58,60,61]. For maximal discrimination an *E. coli* DH5α was included in the test panel since it produced β-glucuronidase, but not β-galactosidase (see Table 3).

Therefore, the combined detection of these two enzyme activities may enable the discrimination of the particular *E. coli* strains tested here.

Table 3
Bacterial enzyme activities determined with enzyme sensing hydrogels.**

Strain	Enzyme activities (based on the literature)			Enzyme activities (experimental results from this study)		
	α-glu	β-gal	β-gus	α-glu	β-gal	β-gus
S. aureus RN4220, **MRSA** N315	+ [52]	- [57]	- [57,81]	+	-	-
EHEC E32511	- [65] *	+ [57]	- [57]	-	+	-
E. coli DH5α	+ [63]	- [62]	+ [57]	+	-	+

α-glu: α-glucosidase, β-gus: β-glucuronidase, β-gal: β-galactosidase;

Enzyme production confirmed (+) for *S. aureus*, MRSA, *E. coli* or EHEC or excluded (-) based on literature data;

Green marked area with +: positive signal (dye released from the specific enzyme responsive hydrogel)

Red marked area with -: negative signal (no dye released from the hydrogel)

* EHEC EDL933 mentioned in [65] is a prototypic O157:H7 EHEC strain.

** The sensing hydrogels showed no signals in bacteria-free LB controls (**Figure S9**a-c).

In addition, *S. aureus*, as another relevant organism that can also provoke food poisoning [54], was tested here via detection of its characteristic enzyme, i.e. α-glucosidase [49,52]. The dye released during the enzymatic reaction was further analyzed in a microplate reader, as shown in Fig. 5. Different responses for the detection of one bacterium with three different enzyme sensing hydrogels are shown in each row. The responses from the same enzyme sensing hydrogel with the two strains of each of the two bacterial species (*E. coli* and *S. aureus*) are shown in each column.

3.5. Enzymatic reactions of enzyme sensing hydrogels in S. aureus suspensions

The monotonic increase of I_F at about 450 nm (λ_{ex} of 365 nm) in Fig. 5a was associated to the formation of deprotonated free 4-MU during the reaction of the α-glucosidase sensing hydrogels in suspensions of both *S. aureus* RN4220 and MRSA N315. The released 4-MU clearly revealed the presence of α-glucosidase in the tested *S. aureus* suspension, since 4-MU was only released from α-glucosidase sensing hydrogels in the presence of α-glucosidase, according to the results in Fig. 2 and Figure S3. These observation are in full agreement with the literature [52].

The apparent rate for the formation of 4-MU was found to be 0.72 min^{-1} and 0.83 min^{-1} in the first 5 h for MRSA N315 and *S. aureus* RN4220, respectively. According to the apparent rate constant obtained from Figure S3a, the α-glucosidase concentration was approximated to be 0.4 nM and 0.5 nM in the initially applied MRSA N315 and *S. aureus* RN4220 suspensions, respectively. Based on the LOD determined above, the α-glucosidase sensing hydrogel thus should detect MRSA N315 and *S. aureus* RN4220 less than 1 h using a microplate reader and in about 12–14 h by bare eye.

No changes were observed in the UV–vis spectra of both the β-galactosidase (Fig. 5b) and β-glucuronidase (Fig. 5c) sensing hydrogels in *S. aureus* suspension. These observations underpin the absence of detectable β-galactosidase and β-glucuronidase activity in both *S. aureus* suspensions, which is in good agreement with the literature [57,81] (see also Table 3).

3.6. Enzymatic reactions of enzyme sensing hydrogels in E. coli suspensions

EHEC E32511 detection. The fluorescence spectra of EHEC E32511 suspensions and the β-glucosidase sensing hydrogel incubated with EHEC E32511 in Fig. 5d did not show any signs of release of 4-MU, since no clear peak at 450 nm was observed after 24 h reaction of the hydrogel in bacterial suspension. Hence the EHEC E32511 suspensions were β-glucosidase negative, in good agreement with the literature [65]. The two broad signals, which are higher in intensity for the hydrogel free condition (bacteria suspension alone), were very likely caused by light scattering by the bacteria and the differences may have resulted from either different numbers of initially applied bacteria in the wells or by an inhibition effect of the hydrogel on EHEC E32511 growth.

By contrast, the absorbance at 615 nm was observed to continuously increase as a function of time both in presence and in absence of the β-galactosidase sensing hydrogel (Fig. 5e). This observation points to an increasing effect of scattering associated to increased numbers of bacteria in all wells (in the absence of fresh nutrition this is tentatively attributed to the adaption of bacteria in the new environment, such as different temperature or oxygen levels). However, after incubation for 7 h, the absorbance for the bacteria suspension alone reached a plateau, while the absorbance for the bacterial suspensions with the hydrogel continued to increase further. Also the spectra recorded after (inset in Fig. 5e) clearly show the absorbance attributed to the dimerized indigo derivative exclusively for the β-galactosidase sensing hydrogel. This observation suggests the presence of β-galactosidase in the suspension of EHEC E32511, since the indigo dye was released from the hydrogel only

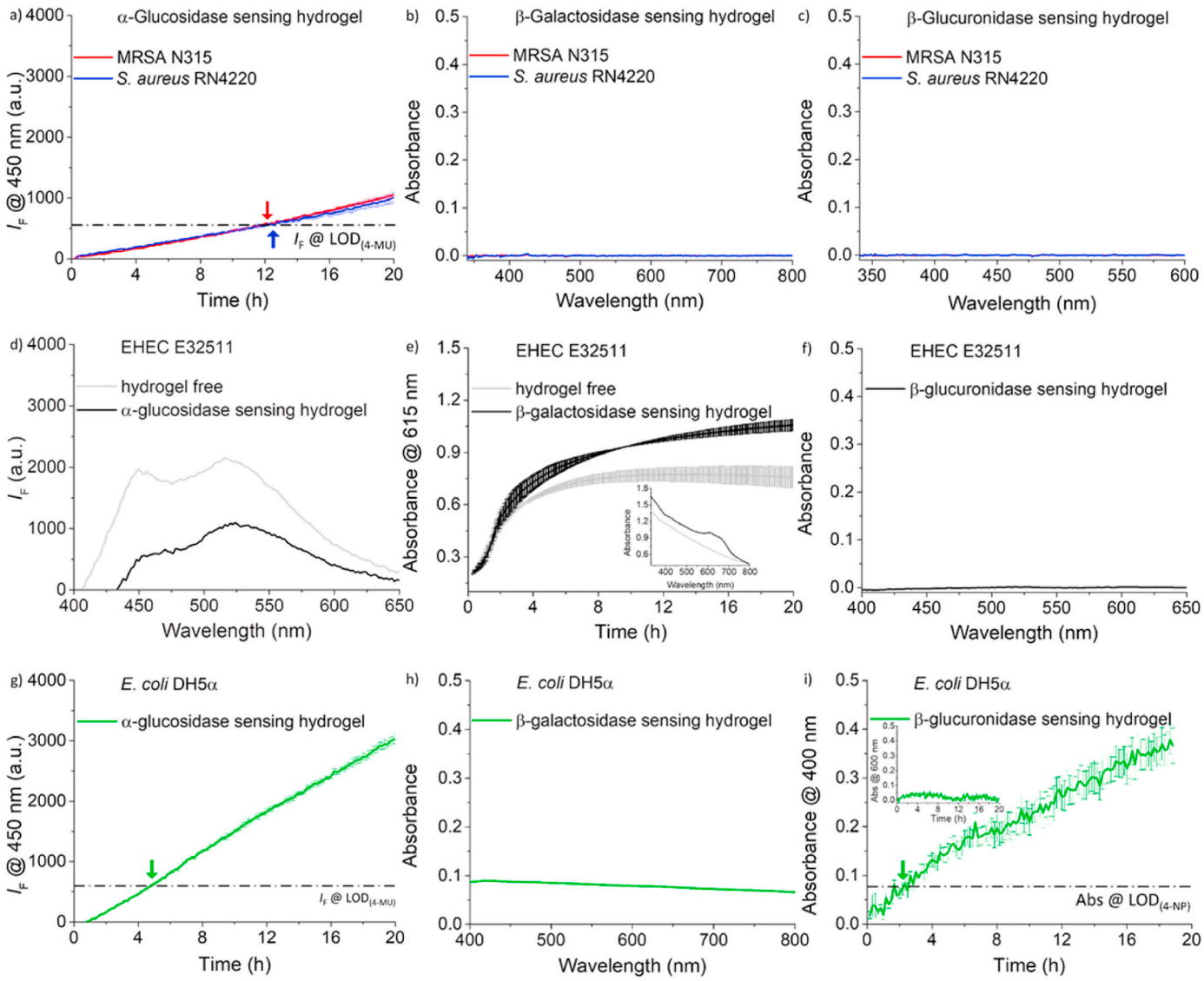

Fig. 5. Detection of enzymes in bacterial suspensions with enzyme sensing hydrogels in a microplate reader format at 25 °C (1st row: detection of *S. aureus* RN4220 (~8×10^9 CFU/mL) and MRSA N315 (~2×10^9 CFU/mL), 2nd and 3rd rows: detection of EHEC E32511 (~6×10^8 CFU/mL), and *E. coli* DH5α (~3×10^9 CFU/mL), respectively. 1st, 2nd and 3rd columns: Measurements with α-glucosidase, β-galactosidase, and β-glucuronidase sensing hydrogels, respectively): a) I_F at maximum emission λ_{max} = 450 nm versus reaction time of α-glucosidase sensing hydrogel incubated with suspensions of *S. aureus* RN4220 and MRSA N315 (biological triplicates). b) and c) Calibrated UV–vis spectra of released indigo and 4-NP in β-galactosidase and β-glucuronidase sensing hydrogels, respectively, incubated with suspension of *S. aureus* RN4220 and MRSA N315; (spectra were corrected according to the spectra of the corresponding dye in Fig. 2) (biological duplicates). d) Fluorescence spectra of the neat cultured EHEC E32511 suspension (i.e. using a hydrogel free well) as well as of the released 4-MU in a α-glucosidase sensing hydrogel incubated with EHEC E32511 (technical replicates). e) Absorbance at λ = 615 nm versus time for the reaction of the β-galactosidase sensing hydrogel in EHEC E32511 as well as the growth curve of pure cultured bacterial suspension in the absence of hydrogel. Kinetics measurement repeat interval: 1.5 min. Insets of e) UV–vis spectra of pure EHEC E32511 suspension and released indigo after 20 h of enzymatic reaction of the hydrogel in the EHEC E32511 (biological duplicates). f) UV–vis spectrum of released 4-NP in β-glucuronidase sensing hydrogel in EHEC E32511 suspension (technical replicates). g) I_F at λ_{max} = 450 nm versus reaction time of α-glucosidase sensing hydrogel incubated with *E. coli* DH5α (biological triplicates). h) UV–vis spectrum of released indigo in β-galactosidase sensing hydrogel in *E. coli* DH5α (biological duplicates). i) Absorbance at λ_{max} = 400 nm versus time for the reaction of hydrogel in *E. coli* DH5α. Inset of i) Absorbance at wavelength λ = 600 nm versus time for the reaction of β-glucuronidase sensing hydrogel in *E. coli* DH5α. Kinetics measurement repeat interval: 10 min (biological triplicates). All spectra in b, c, d, f, h) were acquired after 24 h reaction of the hydrogel in bacterial suspension. Baseline subtraction: Kinetics measurements in a, g, i) I_F or absorbance of corresponding bacteria suspension cultured in sensing hydrogel-free wells; Kinetics measurements in e) Absorbance or UV–Vis spectra of LB for hydrogel free wells as well as absorbance or UV–Vis spectra of sensor hydrogels incubated in LB; Spectra measurement in f, h) UV–vis spectra of corresponding bacteria suspension cultured in sensing hydrogel free wells; spectra measurement in d) and insets of e) Fluorescence/UV-spectra of LB in sensing hydrogel filled well or sensing hydrogel free well for the curve of bacterial suspensions in hydrogel as well as bacterial suspensions in hydrogel free well, respectively. (100 μL of LB or bacterial suspensions, for a, d, g) $[MUD]_{mod}$ = 2.5 mM, λ_{ex} = 365 nm b, e, h) $[X\text{-}Gal]_{mod}$ = 2.5 mM c, f, i) $[PNPG]_{mod}$ = 10 mM). The vertical arrows in a, g, i) point out the time that was required to be able to detect the released dye at the determined LOD by bare eye. Hydrogel free well means the well contained only bacteria suspension.

in the presence of β-galactosidase (compare Fig. 2c and Figure S4). According to the Manual of the Clinical Microbiology, EHEC strains like most *E. coli* strains indeed produce β-galactosidase [57]. Based on the data recorded here, EHEC E32511 should be detectable with the β-galactosidase hydrogel in less than 1.5 h using a microplate reader and in about 8 h by bare eye, according to the previous determined LOD values of indigo dye.

The absence of any absorbance at 400 nm in Fig. 5f shows the absence of β-glucuronidase (compare Fig. 2e and Figure S5), in accordance with reports that concluded that whereas most EHEC strains lack β-glucuronidase [58,60,61], whereas more than 98% of *E. coli* strains exhibit the enzyme.

E. coli DH5α detection. During the enzymatic reaction of the α-glucosidase sensing hydrogel in *E. coli* DH5α suspension (Fig. 5g) a monotonic increase of I_F at about 450 nm was observed due to the released 4-MU. This indicates the presence of α-glucosidase in the tested *E. coli* DH5α suspensions (compare Fig. 2a and S3), that is according to the literature also produced by other *E. coli* strains [63]. The formation of deprotonated free 4-MU occurred with an apparent rate of 2.5 min^{-1} in the first 5 h of reaction. The apparent rate determined for *E. coli* DH5α is higher than for *S. aureus* strains, which is likely caused by different gene expression levels of α-glucosidase. According to the rate constant obtained from Figure S3b, the α-glucosidase concentration was estimated to be 1.4 nM in the initially applied *E. coli* DH5α suspension. Moreover, based on the previously estimated LOD of 4-MU and the growth rate, blue fluorescence emission can be expected to be detectable in less than 1 h using a microplate reader and approximately 5 h by bare eye.

The β-galactosidase hydrogel showed no significant changes even after reaction for 24 h in the characteristic absorbance between 550–700 nm in the UV–vis spectra in Fig. 5h. Hence *E. coli* DH5α can be concluded to not exhibit any β-galactosidase activity, which is caused by a mutation in *LacZ* in this strain, as stated in the literature [62].

Finally, the β-glucuronidase sensing hydrogels showed evidence for liberation of 4-NP when incubated with *E. coli* DH5α (Fig. 5i, compare Fig. 2e and S5). The absorbance at 400 nm increased with progressing reaction time, which is consistent with the literature stating that *E. coli* DH5α secretes β-glucuronidase [57]. The reaction rate for the formation of 4-NP was found to be 0.00057 min^{-1} in the first 2 h. Based on the rate constant obtained from Figure S5b, the β-glucuronidase concentration was estimated to about 17 nM for the initially applied *E. coli* DH5α suspension. By applying β-glucuronidase sensing hydrogel, *E. coli* DH5α can thus be detected in less than 10 min using a microplate reader and about 2.2 h by bare eye.

Thus the detection and differentiation of the *E. coli* strains tested here, i.e. EHEC E32511 and *E. coli* DH5α, was realized due to the lack of β-glucuronidase activity in EHEC E32511 and its lack of β-galactosidase activity, as well as the β-glucuronidase activity in *E. coli* DH5α utilizing the combination of β-galactosidase and β-glucuronidase sensing hydrogels.

Furthermore, by using the combination of three types of enzyme sensing hydrogels, the *S. aureus* strains (RN4220, N315) as well as EHEC E32511 and *E. coli* DH5α, can be discriminated based on their pattern of produced enzymes via the visualization of different dyes released from the hydrogels after enzymatic cleavage (Table 3). In presence of *S. aureus*, the released 4-MU, which shows blue emission, appeared exclusively in the α-glucosidase hydrogel, while the other two hydrogels remained colorless. Once the dimerized blue indigo was formed in the β-galactosidase sensing hydrogel, the presence of β-galactosidase in EHEC E32511 suspension at concentrations >3.4 nM ($t \leq 60$ min) can be concluded. If the 4-NP, which shows yellow color, as well as 4-MU were released in the β-glucuronidase and α-glucosidase sensing hydrogels, respectively, the presence of *E. coli* DH5α in any mixture of the bacteria strains tested here can be concluded.

According to these results, even if other *E. coli* different to *E. coli* DH5α were able to produce β-galactosidase in addition to β-glucuronidase, which is standard for most *E. coli* strains, they can be differentiated from the other bacterial strains tested as well in this study by applying the combination of the three reporter hydrogels, since the three types of enzyme sensing hydrogels can provide another four types of different readouts combination to specify bacteria. Clearly, it is not possible to differentiate all of the test strains, if only one type of enzyme sensing hydrogel is applied, due to the fact that each bacterium produces several bacterial enzymes and each enzyme can also be produced by different bacteria. Especially for the analysis of real samples with higher complexity in a specific setting, it is required to identify more bacterial species in combination. Correspondingly, complex enzyme secretion patterns generated by those bacteria can be present. Hence, a massively multiplexed bacterial sensing approach that combines different enzyme sensing hydrogels as a bottom-up strategy of the detection approach described would be an essential step towards application. Indeed, a data base of bacteria enzyme secretion pattern for each bacterium is necessary to be established to offer a reasonable investigation of new enzyme sensing hydrogel.

A strategy to improve the sensitivity of the system, in particular the bare eye detection, would be to use brighter fluorophores as well as to enlarge the specific surface area or increase the temperature to 37 °C, which may further accelerate the initial reaction rate in the beginning phase of the enzymatic reaction as the reactions start at the surface of the hydrogel. Combined with higher substrate grafting efficiency on the surface of hydrogels this will both accelerate the sensor response and the sensitivity. Additionally, the integration of the enzyme-sensing hydrogels into an automated and sensitive read-out device for point-of-care application would be beneficial for a standardized objectified usage for future applications. Furthermore, physical encapsulation of enzyme substrate into hydrogel with the advantage that the loading of the substrate could be easily varied may shorten the time of bare eye detection, i.e. adding more enzyme substrate in the hydrogel [51].

The hydrogel based detection system showed a good performance in detection of bacterial enzymes and differentiation amongst certain bacteria in a very defined model system tested here, clearly showing the promising potential of the developed detection system. For all future application settings and different sample matrices, the detection approach has to be validated because each detection environment might result in different LODs or ratios of false positive signals.

4. Conclusion

Color-encoded autonomously sensing hydrogels were explored successfully for the sensitive and specific detection of three different bacterial enzymes, i.e. α-glucosidase, β-galactosidase, and β-glucuronidase, which are differentially produced by the four test strains, namely the *S. aureus* lab strain RN4220 and the MRSA strain N315, and the *E. coli* lab strain DH5α and the food-borne pathogenic EHEC, by different colors in a multiplexed pattern format. In particular, the hydrogels were able to detect within 60 min α-glucosidase, β-galactosidase and β-glucuronidase with values of the LODs of 0.2 nM, 3.4 nM and 4.5 nM, respectively, using a conventional microplate reader, as well as LODs of 5.5 nM, 19.6 nM and 35.8 nM by bare eye detection under appropriate illumination. Compared to previously reported systems, our color-encoded system shows a higher sensitivity to the relevant enzymes. Additionally, the hydrogels allow one to distinguish among the different tested bacterial species, i.e. *S. aureus* and *E. coli*, and strains within the same species (EHEC from *E. coli* DH5α), via a color change detectable in less than 1.5 h using a microplate reader and in less than 14 h by bare eye. In the future, the sensing hydrogels reported here can be further optimized and the multiplexing approach expanded for the development of detection and identification systems for specific bacterial strains.

Funding

This work was supported by the European Research Council (ERC

grant to HS, grant No. 279202), the German Academic Exchange Service (DAAD) with financial support of the Bundesministerium für Bildung und Forschung (BMBF), DAAD PPP Frankreich (Projekt-ID 55976814), the Equality Office of the University of Siegen, the Max-Buchner-Forschungsstiftung-Dechema (MBFSt-Kennziffer: 3671), Ministère de l'Europe et des Affaires Etrangères (MEAE) and Ministère de l'Enseignement Supérieur, de la Recherche et de l'Innovation (MESRI; PHC PROCOPE 2017, Project no. 37733UM), SFR SCINBIOS/IBSAM (Brest - France) and association Gaetan Saleun (Brest - France) and the University of Siegen.

CRediT authorship contribution statement

Zhiyuan Jia: Conceptualization, Methodology, Investigation, Formal analysis, Data curation, Writing – original draft. **Mareike Müller:** Methodology, Investigation, Writing – review & editing, Funding acquisition, Resources. **Tony Le Gall:** Investigation, Writing – review & editing, Funding acquisition, Resources. **Martijn Riool:** Investigation, Writing – review & editing. **Max Müller:** Investigation. **Sebastian A.J. Zaat:** Writing – review & editing, Resources. **Tristan Montier:** Funding acquisition, Resources, Writing – review & editing. **Holger Schönherr:** Conceptualization, Funding acquisition, Resources, Project administration, Supervision, Writing – review & editing.

Declaration of competing interest

The authors declare that they have no known competing financial interests or personal relationships that could have appeared to influence the work reported in this paper.

Acknowledgments

The authors thank Dr. Qimeng Song and Dr. Sergey I. Druzhinin for their help with the data analyses and stimulating discussions, Prof. Dr. Constance Schultsz (Amsterdam UMC) for kindly providing the *E. coli* E32511 (EHEC) strain, and Kawaljit Kaur and Sandya Sharma for their assistance in additional microbiological lab work and swelling tests.

Appendix A. Supplementary data

Supplementary data to this article can be found online at https://doi.org/10.1016/j.bioactmat.2021.04.022.

References

[1] WHO, Media Centre. News Release. WHO Publishes List of Bacteria for Which New Antibiotics Are Urgently Needed, 2017 [cited 2020 Dec.], http://www.who.int/mediacentre/news/releases/2017/bacteria-antibiotics-needed/en/.

[2] J.M.A. Blair, M.A. Webber, A.J. Baylay, D.O. Ogbolu, L.J.V. Piddock, Molecular mechanisms of antibiotic resistance, Nat. Rev. Microbiol. 13 (2015) 42–51, https://doi.org/10.1038/nrmicro3380.

[3] Chaired by J. O'NEILL, Tackling Drug-Resistant Infections Globally: Final Report and Recommendations, Government of the United Kingdom, 2016 doi.org/APO-63983.

[4] T. Le Gall, G. Lemercier, S. Chevreux, K.S. Tücking, J. Ravel, F. Thétiot, U. Jonas, H. Schönherr, T. Montier, Ruthenium(II) polypyridyl complexes as photosensitizers for antibacterial photodynamic therapy: a structure-activity study on clinical bacterial strains, ChemMedChem 13 (2018) 2229–2239, https://doi.org/10.1002/cmdc.201800392.

[5] E.J. Culp, N. Waglechner, W. Wang, A.A. Fiebig-Comyn, Y.P. Hsu, K. Koteva, D. Sychantha, B.K. Coombes, M.S. Van Nieuwenhze, Y.V. Brun, G.D. Wright, Evolution-guided discovery of antibiotics that inhibit peptidoglycan remodelling, Nature 578 (2020) 582–587, https://doi.org/10.1038/s41586-020-1990-9.

[6] L. Váradi, J.L. Luo, D.E. Hibbs, J.D. Perry, R.J. Anderson, S. Orenga, P. W. Groundwater, Methods for the detection and identification of pathogenic bacteria: past, present, and future, Chem. Soc. Rev. 46 (2017) 4818–4832, https://doi.org/10.1039/c6cs00693k.

[7] O. Lazcka, F.J. Del Campo, F.X. Muñoz, Pathogen detection: a perspective of traditional methods and biosensors, Biosens. Bioelectron. 22 (2007) 1205–1217, https://doi.org/10.1016/j.bios.2006.06.036.

[8] R. Singh, M.D. Mukherjee, G. Sumana, R.K. Gupta, S. Sood, B.D. Malhotra, Biosensors for pathogen detection: a smart approach towards clinical diagnosis, Sens. Actuators, B 197 (2014) 385–404, https://doi.org/10.1016/j.snb.2014.03.005.

[9] L.D. Renner, J. Zan, L.I. Hu, M. Martinez, P.J. Resto, A.C. Siegel, C. Torres, S. B. Hall, T.R. Slezak, T.H. Nguyen, D.B. Weibel, Detection of ESKAPE bacterial pathogens at the point of care using isothermal DNA-based assays in a portable degas-actuated microfluidic diagnostic assay platform, Appl. Environ. Microbiol. 83 (2017), https://doi.org/10.1128/AEM.02449-16 e0249-16.

[10] A. Mobed, B. Baradaran, M.d. La Guardia, M. Agazadeh, M. Hasanzadeh, M. A. Rezaee, J. Mosafer, A. Mokhtarzadeh, M.R. Hamblin, Advances in detection of fastidious bacteria: from microscopic observation to molecular biosensors, TrAC Trends Anal. Chem. (Reference Ed.) 113 (2019) 157–171, https://doi.org/10.1016/j.trac.2019.02.012.

[11] A.R. Akram, S.V. Chankeshwara, E. Scholefield, T. Aslam, N. McDonald, A. Megia-Fernandez, A. Marshall, B. Mills, N. Avlonitis, T.H. Craven, A.M. Smyth, D.S. Collie, C. Gray, N. Hirani, A.T. Hill, J.R. Govan, T. Walsh, C. Haslett, M. Bradley, K. Dhaliwal, In situ identification of Gram-negative bacteria in human lungs using a topical fluorescent peptide targeting lipid A, Sci. Transl. Med. 10 (2018) 1–12, https://doi.org/10.1126/scitranslmed.aal0033.

[12] H. Li, J. Zhu, Differentiating antibiotic-resistant staphylococcus aureus using secondary electrospray ionization tandem mass spectrometry, Anal. Chem. 90 (2018) 12108–12115, https://doi.org/10.1021/acs.analchem.8b03029.

[13] J.L. Moore, R.M. Caprioli, E.P. Skaar, Advanced mass spectrometry technologies for the study of microbial pathogenesis, Curr. Opin. Microbiol. 19 (2014) 45–51, https://doi.org/10.1016/j.mib.2014.05.023.

[14] M. Lukumbuzya, M. Schmid, P. Pjevac, H. Daims, A multicolor fluorescence in situ hybridization approach using an extended set of fluorophores to visualize microorganisms, Front. Microbiol. 10 (2019) 1383, https://doi.org/10.3389/fmicb.2019.01383.

[15] T. Mocan, C.T. Matea, T. Pop, O. Mosteanu, A.D. Buzoianu, C. Puia, C. Iancu, L. Mocan, Development of nanoparticle-based optical sensors for pathogenic bacterial detection, J. Nanobiotechnol. 15 (2017) 25, https://doi.org/10.1186/s12951-017-0260-y.

[16] H. Peng, I.A. Chen, Rapid colorimetric detection of bacterial species through the capture of gold nanoparticles by chimeric phages, ACS Nano 13 (2019) 1244–1252, https://doi.org/10.1021/acsnano.8b06395.

[17] C.Y. Zhang, J. Gao, Z. Wang, Bioresponsive nanoparticles targeted to infectious microenvironments for sepsis management, Adv. Mater. Weinheim. 30 (2018), e1803618, https://doi.org/10.1002/adma.201803618.

[18] R. Sum, M. Swaminathan, S.K. Rastogi, O. Piloto, I. Cheong, Beta-hemolytic bacteria selectively trigger liposome lysis, enabling rapid and accurate pathogen detection, ACS Sens. 2 (2017) 1441–1451, https://doi.org/10.1021/acssensors.7b00333.

[19] S. Milo, N.T. Thet, D. Liu, J. Nzakizwanayo, B.V. Jones, A.T.A. Jenkins, An in-situ infection detection sensor coating for urinary catheters, Biosens. Bioelectron. 81 (2016) 166–172, https://doi.org/10.1016/j.bios.2016.02.059.

[20] S. Haas, N. Hain, M. Raoufi, S. Handschuh-Wang, T. Wang, X. Jiang, H. Schönherr, Enzyme degradable polymersomes from hyaluronic acid-block-poly (ε-caprolactone) copolymers for the detection of enzymes of pathogenic bacteria, Biomacromolecules 16 (2015) 832–841, https://doi.org/10.1021/bm501729h.

[21] Y. Li, X. Hu, D. Ding, Y. Zou, Y. Xu, X. Wang, Y. Zhang, L. Chen, Z. Chen, W. Tan, In situ targeted MRI detection of Helicobacter pylori with stable magnetic graphitic nanocapsules, Nat. Commun. 8 (2017) 15653, https://doi.org/10.1038/ncomms15653.

[22] C.-K. Joung, H.-N. Kim, M.-C. Lim, T.-J. Jeon, H.-Y. Kim, Y.-R. Kim, A nanoporous membrane-based impedimetric immunosensor for label-free detection of pathogenic bacteria in whole milk, Biosens. Bioelectron. 44 (2013) 210–215, https://doi.org/10.1016/j.bios.2013.01.024.

[23] Y. Tang, Z. Li, Q. Luo, J. Liu, J. Wu, Bacteria detection based on its blockage effect on silicon nanopore array, Biosens. Bioelectron. 79 (2016) 715–720, https://doi.org/10.1016/j.bios.2015.12.109.

[24] P.M. Shaibani, H. Etayash, K. Jiang, A. Sohrabi, M. Hassanpourfard, S. Naicker, M. Sadrzadeh, T. Thundat, Portable nanofiber-light addressable potentiometric sensor for rapid Escherichia coli detection in orange juice, ACS Sens. 3 (2018) 815–822, https://doi.org/10.1021/acssensors.8b00063.

[25] J.P. Yapor, A. Alharby, C. Gentry-Weeks, M.M. Reynolds, A.K.M.M. Alam, Y.V. Li, Polydiacetylene nanofiber composites as a colorimetric sensor responding to Escherichia coli and pH, ACS Omega 2 (2017) 7334–7342, https://doi.org/10.1021/acsomega.7b01136.

[26] H. Zhang, J. Lv, Z. Jia, Detection of ammonia-oxidizing bacteria (AOB) using a porous silicon optical biosensor based on a multilayered double Bragg mirror structure, Sensors (Basel) 18 (2018) 105, https://doi.org/10.3390/s18010105.

[27] Y. Zhang, L. Zhang, L. Yang, C.I. Vong, K.F. Chan, W.K.K. Wu, T.N.Y. Kwong, N.W. S. Lo, M. Ip, S.H. Wong, J.J.Y. Sung, P.W.Y. Chiu, L. Zhang, Real-time tracking of fluorescent magnetic spore–based microrobots for remote detection of C. diff toxins, Sci. Adv. 5 (2019), https://doi.org/10.1126/sciadv.aau9650 eaau9650.

[28] V. Templier, T. Livache, S. Boisset, M. Maurin, S. Slimani, R. Mathey, Y. Roupioz, Biochips for direct detection and identification of bacteria in blood culture-like conditions, Sci. Rep. 7 (2017) 9457, https://doi.org/10.1038/s41598-017-10072-z.

[29] W. Lee, D. Kwon, W. Choi, G.Y. Jung, S. Jeon, 3D-printed microfluidic device for the detection of pathogenic bacteria using size-based separation in helical channel with trapezoid cross-section, Sci. Rep. 5 (2015) 7717, https://doi.org/10.1038/srep07717.

[30] Z. Altintas, M. Akgun, G. Kokturk, Y. Uludag, A fully automated microfluidic-based electrochemical sensor for real-time bacteria detection, Biosens. Bioelectron. 100 (2018) 541–548, https://doi.org/10.1016/j.bios.2017.09.046.

[31] M. Xiao, K. Zou, L. Li, L. Wang, Y. Tian, C. Fan, H. Pei, Stochastic DNA walkers in droplets for super-multiplexed bacterial phenotype detection, Angew. Chem. Int. Ed. 58 (2019) 15448–15454, https://doi.org/10.1002/anie.201906438.
[32] H. Yu, M. Xiao, W. Lai, M.F. Alam, W. Zhang, H. Pei, Y. Wan, L. Li, A self-calibrating surface-enhanced Raman scattering-active system for bacterial phenotype detection, Anal. Chem. 92 (2020) 4491–4497, https://doi.org/10.1021/acs.analchem.9b05614.
[33] H. Yang, M. Xiao, W. Lai, Y. Wan, L. Li, H. Pei, Stochastic DNA dual-walkers for ultrafast colorimetric bacteria detection, Anal. Chem. 92 (2020) 4990–4995, https://doi.org/10.1021/acs.analchem.9b05149.
[34] M.M. Ali, C.L. Brown, S. Jahanshahi-Anbuhi, B. Kannan, Y. Li, C.D.M. Filipe, J. D. Brennan, A printed multicomponent paper sensor for bacterial detection, Sci. Rep. 7 (2017) 12335, https://doi.org/10.1038/s41598-017-12549-3.
[35] Z.A. Islamy Mazrad, I. In, K.-D. Lee, S.Y. Park, Rapid fluorometric bacteria detection assay and photothermal effect by fluorescent polymer of coated surfaces and aqueous state, Biosens. Bioelectron. 89 (2017) 1026–1033, https://doi.org/10.1016/j.bios.2016.10.027.
[36] Z. Li, R. Paul, T. Ba Tis, A.C. Saville, J.C. Hansel, T. Yu, J.B. Ristaino, Q. Wei, Non-invasive plant disease diagnostics enabled by smartphone-based fingerprinting of leaf volatiles, Native Plants 5 (2019) 856–866, https://doi.org/10.1038/s41477-019-0476-y.
[37] A.C. Marques, L. Santos, M.N. Costa, J.M. Dantas, P. Duarte, A. Gonçalves, R. Martins, C.A. Salgueiro, E. Fortunato, Office paper platform for bioelectrochromic detection of electrochemically active bacteria using tungsten trioxide nanoprobes, Sci. Rep. 5 (2015) 9910, https://doi.org/10.1038/srep09910.
[38] A. Pal, D. Goswami, H.E. Cuellar, B. Castro, S. Kuang, R.V. Martinez, Early detection and monitoring of chronic wounds using low-cost, omniphobic paper-based smart bandages, Biosens. Bioelectron. 117 (2018) 696–705, https://doi.org/10.1016/j.bios.2018.06.060.
[39] J. Zhou, S. Hou, L. Li, D. Yao, Y. Liu, A.T.A. Jenkins, Y. Fan, Theranostic infection-responsive coating to in situ detect and prevent urinary catheter blockage, Adv. Mater. Interfaces 5 (2018) 1801242, https://doi.org/10.1002/admi.201801242.
[40] M. Laabei, W.D. Jamieson, R.C. Massey, A.T.A. Jenkins, Staphylococcus aureus interaction with phospholipid vesicles—a new method to accurately determine accessory gene regulator (agr) activity, PLos One 9 (2014), e87270, https://doi.org/10.1371/journal.pone.0087270.
[41] P. Mostafalu, A. Tamayol, R. Rahimi, M. Ochoa, A. Khalilpour, G. Kiaee, I.K. Yazdi, S. Bagherifard, M.R. Dokmeci, B. Ziaie, S.R. Sonkusale, A. Khademhosseini, Smart bandage for monitoring and treatment of chronic wounds, Small 14 (2018) 1703509, https://doi.org/10.1002/smll.201703509.
[42] V. Compernolle, G. Verschraegen, G. Claeys, Combined use of Pastorex Staph-Plus and either of two new chromogenic agars, MRSA ID and CHROMagar MRSA, for detection of methicillin-resistant Staphylococcus aureus, J. Clin. Microbiol. 45 (2007) 154–158, https://doi.org/10.1128/JCM.01115-06.
[43] M. Mimee, P. Nadeau, A. Hayward, S. Carim, S. Flanagan, L. Jerger, J. Collins, S. McDonnell, R. Swartwout, R.J. Citorik, V. Bulović, R. Langer, G. Traverso, A. P. Chandrakasan, T.K. Lu, An ingestible bacterial-electronic system to monitor gastrointestinal health, Science 360 (2018) 915–918, https://doi.org/10.1126/science.aas9315.
[44] L.M. Durso, J.E. Keen, Shiga-toxigenic Escherichia coli O157 and non-Shiga-toxigenic E. coli O157 respond differently to culture and isolation from naturally contaminated bovine faeces, J. Appl. Microbiol. 103 (2007) 2457–2464, https://doi.org/10.1111/j.1365-2672.2007.03473.x.
[45] J.J. Hirvonen, A. Siitonen, S.-S. Kaukoranta, Usability and performance of CHROMagar STEC medium in detection of Shiga toxin-producing Escherichia coli strains, J. Clin. Microbiol. 50 (2012) 3586–3590, https://doi.org/10.1128/JCM.01754-12.
[46] B. Verhaegen, K. de Reu, M. Heyndrickx, L. de Zutter, Comparison of six chromogenic agar media for the isolation of a broad variety of non-o157 shigatoxin-producing Escherichia coli (STEC) serogroups, Int. J. Environ. Res. Publ. Health 12 (2015) 6965–6978, https://doi.org/10.3390/ijerph120606965.
[47] M.-M. Sadat Ebrahimi, Y. Voss, H. Schönherr, Rapid detection of Escherichia coli via Enzymatically triggered reactions in self-reporting chitosan hydrogels, ACS Appl. Mater. Interfaces 7 (2015) 20190–20199, https://doi.org/10.1021/acsami.5b05746.
[48] M.M. Sadat Ebrahimi, H. Schönherr, Enzyme-sensing chitosan hydrogels, Langmuir 30 (2014) 7842–7850, https://doi.org/10.1021/la501482u.
[49] M.-M.S. Ebrahimi, M. Laabei, A.T.A. Jenkins, H. Schönherr, Autonomously sensing hydrogels for the rapid and selective detection of pathogenic bacteria, Macromol. Rapid Commun. 36 (2015) 2123–2128, https://doi.org/10.1002/marc.201500485.
[50] Z. Jia, I. Sukker, M. Müller, H. Schönherr, Selective discrimination of key enzymes of pathogenic and nonpathogenic bacteria on autonomously reporting shape-encodedhydrogel patterns, ACS Appl. Mater. Interfaces 10 (2018) 5175–5184, https://doi.org/10.1021/acsami.7b15147.
[51] Z. Jia, L. Gwynne, A.C. Sedgwick, M. Müller, G.T. Williams, A.T.A. Jenkins, T. James, H. Schönherr, Enhanced colorimetric differentiation between Staphylococcus aureus and Pseudomonas aeruginosa using a shape-encoded sensor hydrogel, ACS Appl. Bio Mater. 3 (2020) 4398–4407, https://doi.org/10.1021/acsabm.0c00403.
[52] J.D. Perry, C. Rennison, L.A. Butterworth, A.L.J. Hopley, F.K. Gould, Evaluation of S. aureus ID, a new chromogenic agar medium for detection of Staphylococcus aureus, J. Clin. Microbiol. 41 (2003) 5695–5698, https://doi.org/10.1128/jcm.41.12.5695-5698.2003.
[53] J.N. Pendleton, S.P. Gorman, B.F. Gilmore, Clinical relevance of the ESKAPE pathogens, Expert Rev. Anti Infect. Ther. 11 (2013) 297–308, https://doi.org/10.1586/eri.13.12.
[54] S. Fooladvand, H. Sarmadian, D. Habibi, A. van Belkum, E. Ghaznavi-Rad, High prevalence of methicillin resistant and enterotoxin gene-positive Staphylococcus aureus among nasally colonized food handlers in central Iran, Eur. J. Clin. Microbiol. Infect. Dis. 38 (2019) 87–92, https://doi.org/10.1007/s10096-018-3398-0.
[55] F.D. Lowy, Staphylococcus aureus infections, N. Engl. J. Med. 339 (1998) 520–532, https://doi.org/10.1056/NEJM199808203390806.
[56] A.S. Meltzer, Medical Laboratory, Manual for tropical countries. Vol. II, Can. Med. Assoc. J. 134 (1986) 1378. PMCID: PMC1491254.
[57] M.A. Pfaller, S.S. Richter, G. Funke, J.H. Jorgensen, M.L. Landry, K.C. Carroll, D. W. Warnock, Manual of Clinical Microbiology, eleventh ed., ASM Press, Washington, DC, USA, 2015.
[58] S.L. Percival, Microbiology of Waterborne Diseases: Microbiological Aspects and Risks, second ed., Elsevier, London, UK, 2014.
[59] A. Leclercq, B. Lambert, D. Pierard, J. Mahillon, Particular biochemical profiles for enterohemorrhagic Escherichia coli O157:H7 isolates on the ID 32E system, J. Clin. Microbiol. 39 (2001) 1161–1164, https://doi.org/10.1128/JCM.39.3.1161-1164.2001.
[60] S. Orenga, A.L. James, M. Manafi, J.D. Perry, D.H. Pincus, Enzymatic substrates in microbiology, J. Microbiol. Methods 79 (2009) 139–155, https://doi.org/10.1016/j.mimet.2009.08.001.
[61] M.-M. Sadat Ebrahimi, Y. Voss, H. Schönherr, Rapid detection of Escherichia coli via enzymatically triggered reactions in self-reporting chitosan hydrogels, ACS Appl. Mater. Interfaces 7 (2015) 20190–20199, https://doi.org/10.1021/acsami.5b05746.
[62] Y. Song, B.-R. Lee, S. Cho, Y.-B. Cho, S.-W. Kim, T.J. Kang, S.C. Kim, B.-K. Cho, Determination of single nucleotide variants in Escherichia coli DH5α by using short-read sequencing, FEMS Microbiol. Lett. 362 (2015) fnv073, https://doi.org/10.1093/femsle/fnv073.
[63] S. Paul, T.K. Chaudhuri, Chaperone mediated solubilization of 69-kDa recombinant maltodextrin glucosidase in Escherichia coli, J. Appl. Microbiol. 104 (2008) 35–41, https://doi.org/10.1111/j.1365-2672.2007.03519.x.
[64] A.U. Kresse, M. Rohde, C.A. Guzmán, The EspD protein of enterohemorrhagic Escherichia coli is required for the formation of bacterial surface appendages and is incorporated in the cytoplasmic membranes of target cells, Infect. Immun. 69 (1999) 4834–4842, https://doi.org/10.1128/IAI.67.9.4834-4842.1999.
[65] K.-H. Oh, S.-H. Cho, Interaction between the quorum sensing and stringent response regulation systems in the enterohemorrhagic Escherichia coli O157:H7 EDL933 strain, J. Microbiol. Biotechnol. 24 (2014) 401–407, https://doi.org/10.4014/jmb.1310.10091.
[66] J.D. Perry, A decade of development of chromogenic culture media for clinical microbiology in an era of molecular diagnostics, Clin. Microbiol. Rev. 30 (2017) 449–479, https://doi.org/10.1128/CMR.00097-16.
[67] M.-M. Sadat Ebrahimi, N. Dohm, M. Müller, B. Jansen, H. Schönherr, Self-reporting hydrogels rapidly differentiate among enterohemorrhagic Escherichia coli (EHEC) and non-virulent Escherichia coli (K12), Eur. Polym. J. 81 (2016) 257–265, https://doi.org/10.1016/j.eurpolymj.2016.06.010.
[68] Z. Jia, M. Müller, H. Schönherr, Towards multiplexed bacteria detection by enzyme responsive hydrogels, Macromol. Symp. 379 (2018) 1600178, https://doi.org/10.1002/masy.201600178.
[69] B.N. Kreiswirth, S. Löfdahl, M.J. Betley, M. O'Reilly, P.M. Schlievert, M.S. Bergdoll, R.P. Novick, The toxic shock syndrome exotoxin structural gene is not detectably transmitted by a prophage, Nature 305 (1983) 709–712, https://doi.org/10.1038/305709a0.
[70] D. Nair, G. Memmi, D. Hernandez, J. Bard, M. Beaume, S. Gill, P. Francois, A. L. Cheung, Whole-genome sequencing of Staphylococcus aureus strain RN4220, a key laboratory strain used in virulence research, identifies mutations that affect not only virulence factors but also the fitness of the strain, J. Bacteriol. 193 (2011) 2332–2335, https://doi.org/10.1128/JB.00027-11.
[71] M. Kuroda, T. Ohta, I. Uchiyama, T. Baba, Y. Yuzawa, I. Kobayashi, L. Cui, A. Oguchi, K. Aoki, Y. Nagai, J. Lian, T. Ito, M. Kanamori, H. Matsumaru, A. Maruyama, H. Murakami, A. Hosoyama, Y. Mizutani-Ui, N.K. Takahashi, T. Sawano, R. Inoue, C. Kaito, K. Sekimizu, H. Hirakawa, S. Kuhara, S. Goto, J. Yabuzaki, M. Kanehisa, A. Yamashita, K. Oshima, K. Furuya, C. Yoshino, T. Shiba, M. Hattori, N. Ogasawara, H. Hayashi, K. Hiramatsu, Whole genome sequencing of meticillin-resistant *Staphylococcus aureus*, Lancet 3571225–1240 (2001), https://doi.org/10.1016/S0140-6736(00)04403-2.
[72] D.M. Woodcock, P.J. Crowther, J. Doherty, S. Jefferson, E. DeCruz, M. Noyer-Weidner, S.S. Smith, M.Z. Michael, M.W. Graham, Quantitative evaluation of Escherichia coli host strains for tolerance to cytosine methylation in plasmid and phage recombinants, Nucleic Acids Res. 17 (1989) 3469–3478, https://doi.org/10.1093/nar/17.9.3469.
[73] G.A. Willshaw, H.R. Smith, S.M. Scotland, A.M. Field, B. Rowe, Heterogeneity of Escherichia coli phages encoding Vero cytotoxins: comparison of cloned sequences determining VT1 and VT2 and development of specific gene probes, J. Gen. Microbiol. 133 (1987) 1309–1317, https://doi.org/10.1099/00221287-133-5-1309.
[74] P. Mukhopadhyay, K. Sarkar, S. Bhattacharya, A. Bhattacharyya, R. Mishra, P. P. Kundu, pH sensitive N-succinyl chitosan grafted polyacrylamide hydrogel for oral insulin delivery, Carbohydr. Polym. 112 (2014) 627–637, https://doi.org/10.1016/j.carbpol.2014.06.045.

[75] C. Yan, D. Chen, J. Gu, H. Hu, X. Zhao, M. Qiao, Preparation of N-succinyl-chitosan and its physical-chemical properties as a novel excipient, J. Pharm. Soc. Jpn. 126 (2006) 789–793, https://doi.org/10.1248/yakushi.126.789.
[76] A. Kumar, G.M. Whitesides, Features of gold having micrometer to centimeter dimensions can be formed through a combination of stamping with an elastomeric stamp and an alkanethiol ‘‘ink’’ followed by chemical etching, Appl. Phys. Lett. 63 (1993) 2002–2004, https://doi.org/10.1063/1.110628.
[77] R.F. Chen, Fluorescent pH indicator. Spectral changes of 4-methylumbelliferone, Anal. Lett. 1 (1968) 423–428, https://doi.org/10.1080/00032716808051147.
[78] Members in Thermo Fisher Scientific Inc., Crosslinkers Technical Handbook, 2012. Printed in the U.S., Reference to a chapter named chemical reactivity of crosslinkers and modification reagents, 4.
[79] J.N. Miller, J.C. Miller, Statistics and Chemometrics for Analytical Chemistry, fifth ed., Pearson Education, Gosport, Hants, UK, 2005, pp. 115–124.
[80] K. Kaur, W. Chelangat, S.I. Druzhinin, N. Wangechi Karuri, M. Müller, H. Schönherr, Quantitative E. coli enzyme detection in reporter hydrogel-coated paper using a smartphone camera, Biosensors 11 (2021) 25, https://doi.org/10.3390/bios11010025.
[81] C. Cotte, S. Orenga, A. Re, Staphylococcus Aureus-specific Detection Media and Identifying And/or Counting Method Using Same, 2004, US20040121404A1.